Human La's nuclear retention element functions in La-RNA target discrimination.

Stefano Marrella

A THESIS SUBMITTED TO FACULTY OF GRADUATE STUDIES IN PARTIAL FULFILMENT OF THE REQUIREMENTS FOR THE DEGREE OF

MASTER OF SCIENCE

GRADUATE PROGRAM IN BIOLOGY

YORK UNIVERSITY

TORONTO, ONTARIO

August 2017

ABSTRACT

The La protein is an abundant RNA processing protein located in the nucleus of eukaryotic cells. Removal of the α-helical nuclear retention element domain in human La causes the inappropriate export of these hLa-ΔNRE mutants from the nucleus, resulting in the accumulation of non-functional aberrantly processed tRNAs within the cytoplasm. We hypothesized that the inappropriate nuclear export of hLa-ΔNRE may be an indirect consequence of altered RNA target binding in cells. Electrophoretic mobility shift assays revealed hLa-ΔNRE mutants exhibiting diminished binding affinity for precursor tRNAs in comparison to wild-type human La, however no differences in affinity were seen with poly A target binding. From this, we proposed a hypothetical model which suggests the cause for export of hLa-ΔNRE mutants is a result of competitive binding with mRNA targets in the nucleus. This competition for binding results in the inappropriate export of these mutants with mRNA targets in a crm1-dependant manner.

ACKNOWLEDGMENTS

I would like to express my sincerest appreciation towards my supervisor Dr. Mark Bayfield for accepting my unique request to complete my Master's thesis in his lab. Your expertise in the field of study, outstanding guidance and consistent positive encouragement have made this entire process not only a phenomenal learning experience but an enjoyable one as well.

I would also like to acknowledge my wonderful lab members Andi, Jyotsna, Ana and Rawaa who were also my family for the past two years. Thank you for training me in various lab techniques and for all your supportive assistance in and outside of the lab. Despite the various roads we all will take in the future, I know I have found friends for life.

Next, I would like to thank my parents and girlfriend for all of their support throughout my journey. You had the patience to hear me express all of my frustrations about failed experiments even though you had no idea as to what I was talking about.

In addition, I would like to thank my advisor Dr. Andy White for accepting this role. Your comments and suggestions during each annual progress report were always taken into consideration when planning future experiments.

Finally, I would like to express my appreciation towards my other committee members Dr. Hudak and Dr. Audette for accepting the responsibility to partake in my defense.

TABLE OF CONTENTS

LIST OF TABLES

LIST OF FIGURES

LIST OF ABBREVIATIONS

3’ UUU-OH: terminal uridylate sequence found at 3’ end of pol III transcripts

ΔNRE E132A D133A: ΔNRE mutant with additional substitution mutations in its RRM1

ΔNRE F150A: ΔNRE mutant with alanine substituted for phenylalanine in its RRM1

CK2: Casein Kinase 2

CLIP: Cross-linking immunoprecipitation assay

Crm1: Chromosome maintenance region 1

DMEM: Dulbecco modified eagle medium

EMSA: Electrophoretic mobility shift assay

FBS: Fetal bovine serum

GFP: Green fluorescent protein

H/D exchange: Hydrogen deuterium exchange mass spectrometry

hLa: Human Lupus autoantigen

hLa-ΔNRE: hLa mutants lacking their nuclear retention element

hLa E132K D133K K316E K317E: Human La with lysines substituted at positons 132 and 133 of RRM1 and glutamates substituted for lysines at positions 316 and 317.

hLa K316E K317E: Human La with glutamates substituted for lysines at positions 316 and 317.

HPLC MS: High pressure liquid chromatography mass spectrometry

HuR: Human antigen R

KK mutant: Human La with alanines substituted for lysines at positions 316 and 317.

La: Lupus autogentigen

LAM: La Motif

LARP: La-related protein

LDB: La dilution buffer

LMB: Leptomycin B

LRPPRC: Leucine-rich pentatricopeptide repeat protein

mRNA: messenger RNA

mRNP: messenger ribonucleoprotein complex

NES: Nuclear export signal

NLS: Nuclear Localization Signal

NPC: Nuclear pore complex

NRE: Nuclear Retention Element

Nxf1: Nuclear export factor 1

Nxf3: Nuclear export factor 3

Nxt1: NTF2-related export protein 1

PABP: Poly A binding protein

PAGE: Polyacrylamide gel electrophoresis

PNK: Proteinase K

Pol III: RNA polymerase III

Pre-tRNA: Precursor tRNA

RACK1: Ribosome-associated receptor for activated C kinase

RNA: Ribonucleic acid

RRM: RNA Recognition Motif

rRNA: ribosomal RNA

SBM: Short Basic Motif

SDS: Sodium dodecyl sulfate

Sla1p: Fission yeast La protein (*S.Pombe*)

snRNA: small nuclear RNA

SS-B: Sjogrens Syndrome antigen B

SSC: Saline sodium citrate

T4 PNK: T4 polynucleotide kinase

TBS: Tris-buffered saline

TBST: Tris-buffered saline + tween

tRNA: transfer RNA

wHTH: winged Helix-Turn-Helix

INTRODUCTION

The Lupus autoantigen commonly known as La is an abundant protein found in nearly all eukaryotes [1]. La is a multidomain protein consisting of 408 amino acids, its domains are separated into a conserved N terminal region and a divergent C terminal region. A human homologue of La was first identified as an autoantigen in patients suffering from autoimmune disorders lupus erythematosus and Sjogren's syndrome [2] giving rise to commonly used names Human La autoantigen (hLa) and Sjogrens syndrome antigen B (SS-B). La is an RNA processing protein found in all metazoans and its presence within higher eukaryotic organisms is essential for their viability [3]. Deletions in fission yeast indicate the presence of La independent mechanisms which maintain their survival [4,5]. The RNA processing activity of La is so highly conserved that human La can replace many processing functions of the fission yeast La protein known as Sla1p [8]. This makes yeast a good study model to help understand La's fundamental roles within the cell.

1.1 La protein structure

The La protein is a member of a large group of RNA binding proteins that contain an RNA recognition motif (RRM) allowing it to bind various RNA substrates [6]. The standard RRM follows a $\beta_1\alpha_1\beta_2\beta_3\alpha_2\beta_4$ topology in which four beta sheets are packed against two alpha helices allowing it to recognize single stranded RNA and engage in post transcriptional processes [9]. La contains an RRM1 in its conserved N terminal region that slightly deviates from the standard topology possessing a $\alpha_o\beta_1\alpha_1\beta_2\beta_3\alpha_2\beta_4\alpha_3$

architecture which includes the addition of an alpha helix (α_0) at the beginning of the domain and an α_3 helix located in La's C-terminal region. Although slight variations in the secondary structural components that make up an RRM exist between different RNA binding proteins the method by which they interact with RNA is largely consistent. Single stranded RNA lying across the four beta sheets interacts with conserved aromatic side groups protruding from these sheets. Hydrophobic stacking interactions between the aromatic side groups and the targeted RNA allow for a stable contact [10].

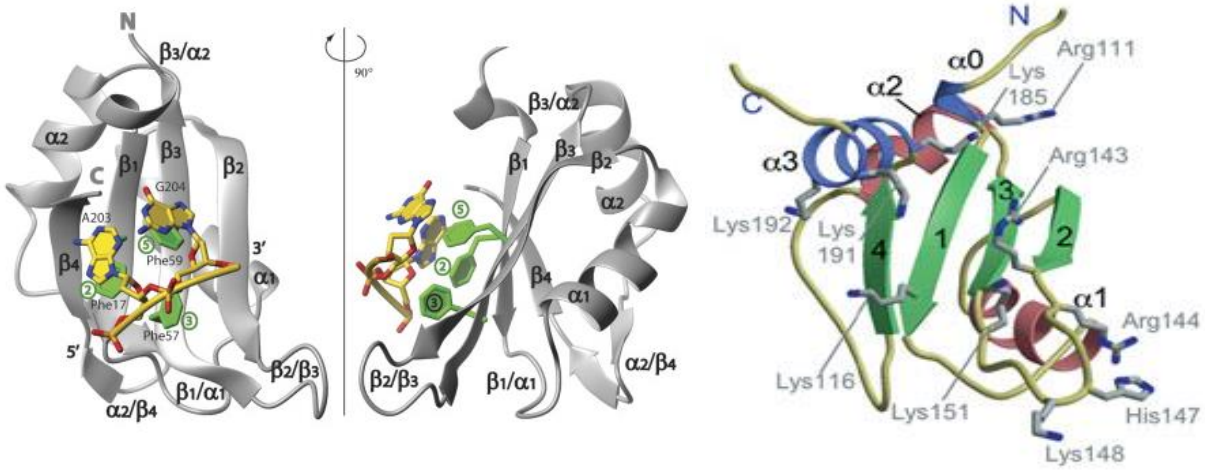

"Standard" RRM hLa RRM1

Figure 1: *Structural representation of a standard RNA recognition motif (left) (PDB ID 1up1) and the first RNA recognition motif found in the NTD of the human lupus autoantigen (PDB ID 1s79). Slight variations in the hLa RRM1 exist in comparison to a standard RRM. These differences include the presence of an α0 helix located near the NTD of hLa's RRM1 as well as an additional α3 helix located near the C terminal region of the RRM1. Despite these differences, interaction with RNA targets is conserved and mediated through aromatic side chain residues protruding from the 4 beta-sheets depicted by the green residues in the standard RRM. Figure adapted from Clery et al 2004 [9] and Alfano et al 2004 [65].*

Along with the RRM1 domain, La also contains a La motif (LAM) which is critical in its binding of RNA substrates. The LAM consists of five alpha helices and three antiparallel beta sheets organized into a winged helix turn helix fold (wHTH) [11]. This structure is commonly found in transcription factors which engage with dsDNA by inserting their recognition helix into the major groove. Other proteins bearing this wHTH fold such as the restriction endonuclease FokI use it for protein-protein interactions [12], this provides evidence for additional targets other than RNA that the La protein could potentially interact with. The LAM together with the RRM1 make up what is called the La module located in the conserved N terminal region of the protein. The binding pocket created by these domains is made possible through a short linker region that separates both domains [25].

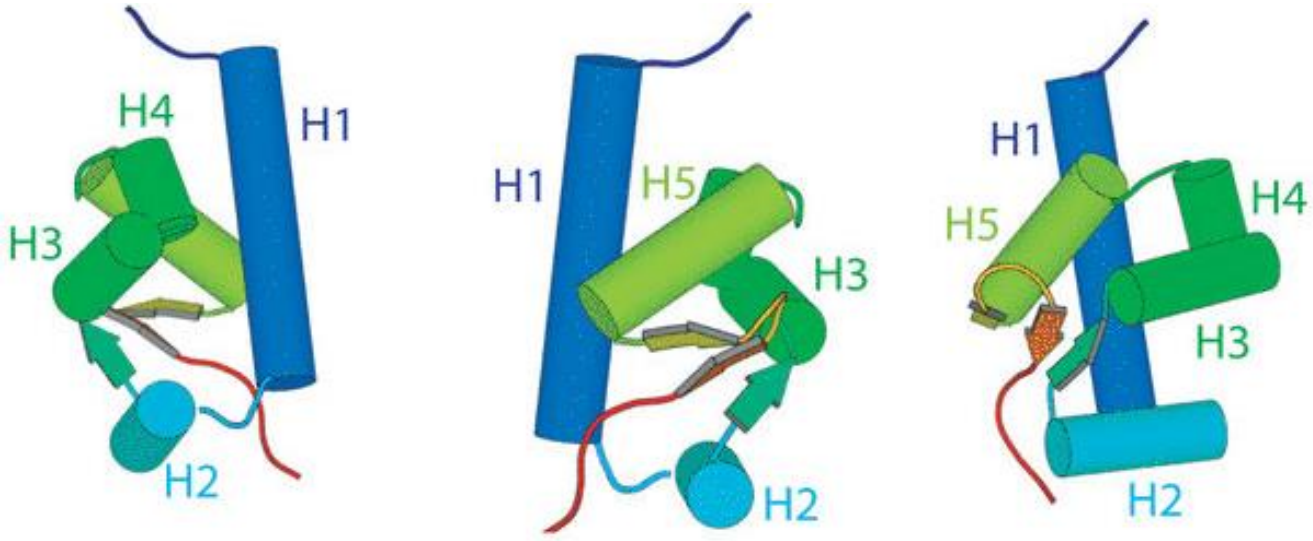

Figure 2: *Structural representation of the La motif seen from three separate angles (PDB ID 1s29). The five alpha helices and three beta sheets the protein domain is comprised of are arranged in a winged Helix turn Helix orientation. Classically, this structural motif is known for interacting with double stranded nucleic acid sequences. The La Motif along with the RRM1 collectively known as the La module form a binding pocket enabling La to interact with its various RNA substrates. This binding pocket is made possible due to a flexible linker region located between the two domains. Figure adapted from Dong et al. 2004* [11]*.*

The C terminal region of La proteins is more divergent than the conserved N terminus and its size increases from yeast to higher organisms [25]. The C terminal domain of human La contains the addition of a second RRM2 which is more commonly present in other higher eukaryotes. Immediately following the RRM2 is a region known as the Nuclear Retention Element (NRE) which has been demonstrated to form an α-helical structure that partially blocks the β_4 canonical RNA binding region of the RRM2 (figure 3) [26]. A short basic motif (SBM) which is only present in human La is located

directly after the NRE. This region is comprised of a Walker-A-like motif and has been shown to decrease hLa's binding affinity for precursor tRNAs (pre-tRNAs) when the serine at position 366 is phosphorylated by casein kinase 2 (CK2) [28]. A Nuclear localization signal (NLS) is located at the end of the C terminus in both yeast and human La. Since La has been known to shuttle between the nucleus and cytoplasm of cells depending on the RNA substrate it is bound to, [27] the NLS allows for La's re-entry into the nucleus [29].

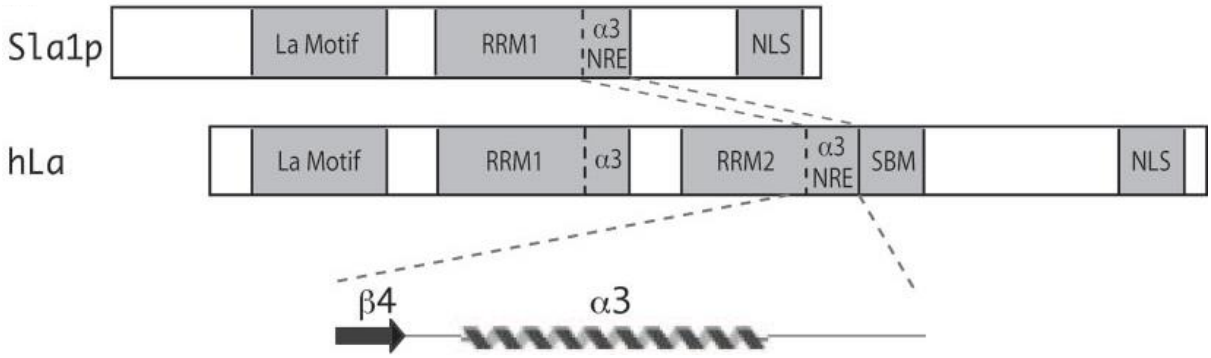

Figure 3: *Schematic diagram illustrating the protein domains that encompass the human lupus autoantigen (hLa) and its yeast homolog (Sla1p). The NTD region of both proteins are highly conserved with each containing both a La motif and an RRM1 motif. Structural divergence begins in the CTD region with hLa possessing and additional RNA recognition motif (RRM2) as well as a short basic motif (SBM). The alpha helical NRE region in hLa is also present directly after the RRM2 whereby its partially blocks access to the β4 sheet of the RRM2. In Sla1p this region immediately succeeds the RRM1. Figure adapted from Bayfield et al 2007 [8].*

1.2 La engages with a variety of RNA binding targets

La preferentially binds to RNA targets ending in stretches of uridylate residues which occur on the ends of all nascent RNA polymerase III (pol III) transcripts [7]. Recognition of the 3' terminal UUU-OH by La is made possible through its interaction with the La module. A crystal structure showcasing the recognition of the termini of nascent RNA Pol III transcripts by the La module specifies interaction of the final three uridylate nucleotides in a splayed apart orientation with the La module (figure 4) [6]. Thus as designated in the cited paper, terminal uridylates U7 and U9 of the 9-mer RNA transcript fold together forming a C shape which allows recognition of U7 and U9 by conserved basic and aromatic residues in the La motif and recognition of U8 by the back bone peptides of β_4 in the RRM1. The La motif contains the bulk of the responsibility for engaging in this poly uridylate binding mode since mutations incorporated into this domain abolish La's recognition of poly uridylate sequences [22]. The interaction between U8 and the RRM1 is interesting because it does not engage in any contact with the conserved basic residues of the RRM1 that were initially hypothesized for recognition. This leaves the unbound RRM1 region open to potential secondary contacts with the same or different RNA substrates.

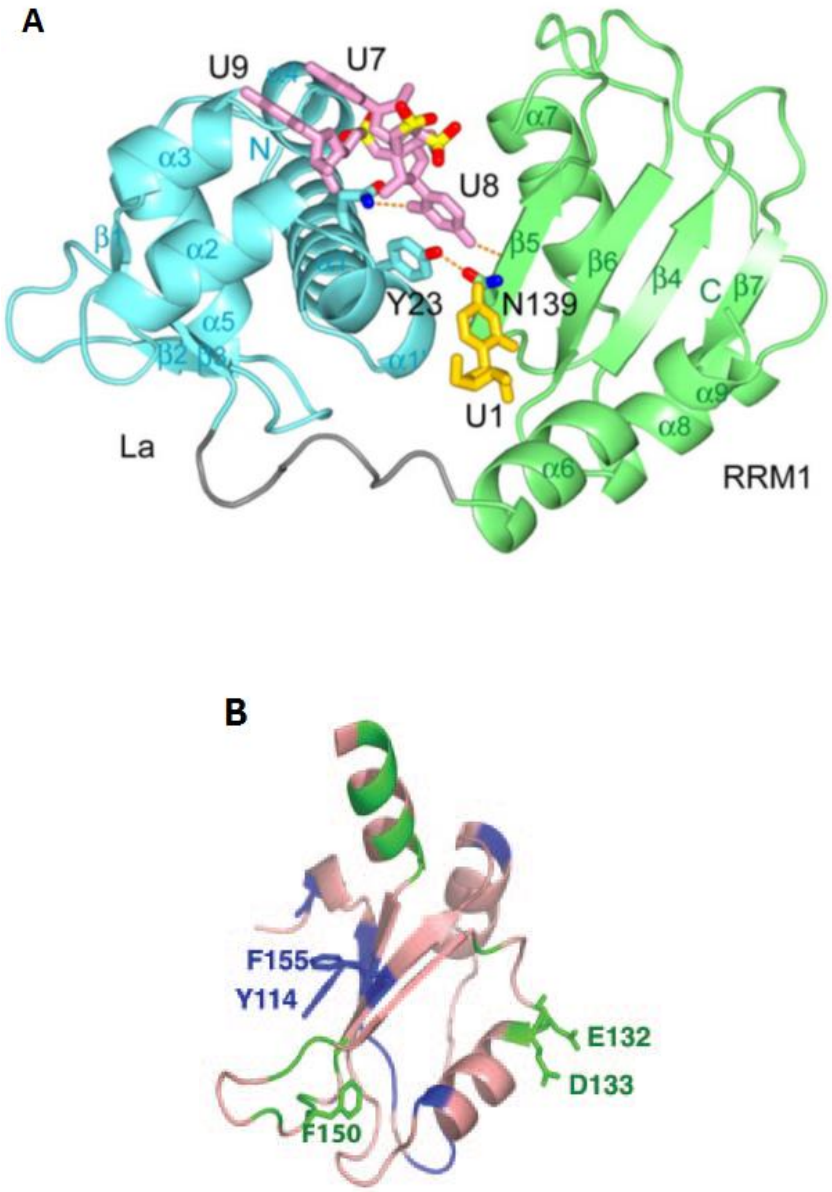

Figure 4: A) *A crystal structural of the La Motif (cyan) and the RRM1 (green) colllectively termed the La module and their interaction with a 9mer RNA oligo (PDB ID 1zh5). The final three nucleotides of the 9mer comprised of uridines interact with the La module in a splayed apart orientation. The U8 nucleotide is critical for this interaction, by making hydrogen bond contacts with both I140 in the β5 sheet of the RRM1 and the amide group of G20 in the α1 helix of the LAM. In addition to this, U8 also interacts with tyrosine 23 of the α1 helix via ring stacking. The U9 nucelotide also makes ring stacking interactions with phenylalanines at positions 35 and 55 on the LAM α2 and α3 helices respectively. The flexible linker region between both domains allowing for the formation of this binding pocket is highlighted in gray. Figure adapted form Teplova et al. 2006* [6]*.* ***B)*** *RRM1 of human La with glutamic acid and aspartic acid residues at positions 132 and 133 respecitively along with phenylalanine at position 150 hilighted in green. Figure adapted from Bayfield et al. 2007* [8]*.*

La has been shown to interact with a variety of RNA Pol III transcripts such as pre-5S rRNA, Y-RNA and 7SK RNA however, its best characterized substrates are pre-tRNAs [13-16]. Binding to these pre-tRNA targets is dependent on the La modules recognition of the 3' terminal oligo U tract along with secondary interactions made between loop 3 of the RRM1 and the tRNA body [22]. The amount of terminal U's present in the pre-tRNA 3' trailer determines La's binding efficiency, for example, human La requires a minimum of 3 terminal U's for binding whereas yeast *S. Pombe* La require 4 or more [7, 17-19]. Preference for La to engage in pre-tRNA binding over poly U binding is dependent on UUU-OH independent interactions mediated by RRM1's loop 3 region which is distinct from the La module binding site. Therefore, La's poly U binding mode is required to recognize the 3' trailer of pre-tRNAs and additional interactions made by the loop 3 of RRM1 stabilize this interaction and increase its affinity. Thus 3' UUU-OH recognition by the La module in conjunction with RRM1 loop 3 interaction with pre-tRNA comprises La's pre-tRNA binding mode.

Recent unpublished data within our lab has shown that along with binding to nascent RNA pol III transcripts, La can also bind to poly A oligomers in a length dependent manner. This interaction is evident using an electrophoretic mobility shift assay (EMSA) also commonly referred to as a gel shift. The RNA substrate in question is radioactively labeled with ^{32}P γ ATP which incorporates the labelled phosphate on the 5' end of the RNA during reverse transcription from cDNA. This radioactively labeled substrate becomes visible when exposed to a phosphor-screen and its migration in a gel is dependent on whether it binds to the protein it is placed with. Free labelled substrate that does not bind to the protein migrates to the bottom of the gel whereas

bound substrate migrates less creating a shift in the band appearance on the gel. The binding mode used to recognize poly A sequences involves the LAM, RRM1 and secondary RRM domain located at the C terminal region in human La known as RRM2. The particular regions within each domain and how each domain interacts with the poly A sequence are currently being investigated, however, it is presently understood that poly A binding occurs at separate sites on the LAM and RRM1 since mutations in the regions were poly U and pre-tRNAs interact with show no alteration of the poly A binding mode. Considering La's extensive role in pre-cursor tRNA processing, research is ongoing to investigate whether La has regulatory functions in the processing of mRNAs, specifically binding to poly A tails and modulating the activity of poly A binding protein (PABP).

1.3 Nuclear export of La's RNA targets

As mentioned earlier, La can interact with a variety of RNA targets such as tRNAs, rRNAs, snRNAs as well as mRNAs primarily through the usage of its LAM, RRM1 and RRM2 binding domains. Although a commonality amongst these RNAs is that they can interact with La, they contain unique differences in their means of export from the nucleus, the general mechanisms of which will be briefly discussed.

1.3.1 mRNA export

There are two major export receptors of mRNA in mammalian cells; The Nuclear export factor 1 (Nxf1) and The Chromosome maintenance region 1 (crm1). Nuclear export via Nxf1 is accomplished by Nxf1 forming a heterodimer with NTF2-related export protein 1 (Nxt1) enabling the interaction with spliced mRNA via the enzyme complex TREX1 (conserved from yeast to humans) [46]. This heterodimer interaction is critical since defective Nxf1 (which can not bind with Nxt1) does not promote mRNA export [47]. After passage of this messenger ribonucleoprotein (mRNP) through the nuclear pore complex (NPC) a conformational change in the mRNP known as "remodelling" occurs which is essential for mRNA dissociation in the cytoplasm and recycling of export factors back into the nucleus. The second major export factor Crm1, is a member of the importin-beta family. Crm1 itself is not an RNA binding protein, instead it requires an adaptor protein to accomplish this task. Crm1 interacts with the nuclear export signal (NES) of its cargo and export is mediated through Ran-GTP [48]. To date, three crm1 adaptor proteins have been identified for the export of mRNAs; RNA binding protein Human antigen R (HuR), Leucine-rich pentatricopeptide repeat protein (LRPPRC) and nuclear export factor 3 (Nxf3). HuR interacts with messenger RNAs containing AU rich elements [49] while LRPPRC engages with mRNAs by directly interacting with eIF4E as well as 4E-SE RNA elements [50]. Nxf3 possesses a Crm1 dependant export signal and can tether mRNA for their export from the nucleus [51]. In light of this, there still remain many RNAs exported by crm1 for which adaptor proteins have not yet been identified [52].

1.3.2 rRNA and snRNA export

In addition to mRNAs, crm1 is also responsible for the nuclear export of rRNAs and snRNAs. Both the pre-60s ribosomal subunit containing 5s, 5.8s and 28s (25s in yeast) rRNA along with the pre-40s subunit containing 18s rRNA are exported in a crm1-dependant manner. Crm1 export of pre-60s ribosomal subunits are mediated through the adaptor protein Nmd3 whereas pre-40s subunits rely on interaction with adaptor proteins Ltv1 and Pno1/Dim2 for crm1 nuclear export [46]. snRNAs are exported from the nucleus via crm1 through the aid of the PHAX adaptor protein which not only binds to crm1 but also the RNA's cap binding complex (CBC) and the 5' end of the snRNA [53]. From this it is evident that crm1 is involved in the export of a variety of different RNA sequences with in the nucleus, however, the type of RNA exported via crm1 is dictated by the distinct adaptor protein with which they interact with.

1.3.3 tRNA export

Currently, the only well known exporter of tRNAs across the NPC is mediated through exportin-T (Xpot) in vertebrates and its homolog Los1 in yeast. Xpot/Los1 are members of the importin-beta family and like crm1, export is regulated by a Ran GTPase. At the present time, Los1 is the only protein known to transport intron-containing pre-tRNAs into the cytoplasm [54] however, the yeast Los1Δ strain is viable. In addition to this, the *Arabidopsis thaliana* plant Xpot homolog PAUSED is non-essential

and insects lack a Xpot homolog [55-59]. Taken together, these data suggest the existence of a novel nuclear exporter for tRNAs. After their transcription and export, tRNAs can contribute to translation in the cytoplasm however, it has been recently determined that tRNAs can undergo retrograde import into the nucleus and that this process is conserved from yeast to humans [60-62]. The biological function of this retrograde import is speculated for additional tRNA modification or tRNA quality control purposes [63,64].

1.4 La's role in the processing and maturation of precursor tRNAs

La promotes the proper processing of pre-tRNAs to mature tRNAs via a mechanism known as simple 3' end binding. La begins the process by binding to the 3' terminal oligo U tract of pre-tRNAs protecting them from degradation of 3' exonuclease Rex1p [20, 21]. The number of uridylate residues at the 3' terminus defines La's binding affinity to the pre-tRNA which in turn dictates whether processing is completed via a La-dependant or La-independent manner (Figure 4). In addition to this 3' end binding, the loop 3 region (amino acids 143-151) of hLa's RRM1 also binds to the body of the pre-tRNA and stabilizes this interaction. Collectively these site separate binding events comprise the pre-tRNA binding mode. La directs the removal of the 5' leader sequence of pre-tRNAs by RNase P to precede 3' trailer processing since in the absence of La this order is reversed in yeast [16]. The 3' end protected pre-tRNA then becomes processed by RNaseZ precisely at the first unpaired nucleotide following the acceptor stem leading to the dissociation of La from the tRNA and the addition of CCA trinucleotide to the new 3' end [22]. Additional chemical modifications to the tRNA are

made during this period prior to its export into the cytoplasm via Los1 in yeast or exportin-t in vertebrates. About 20 percent of all pre-tRNAs contain an intron, and if present, splicing occurs once the precursor tRNA has been exported into the cytoplasm where the pre-tRNA splicing machinery is located on the outer membrane of the mitochondria. La dissociates from the 3' trailer in the nucleus and recycles to re-associate with a new pre-tRNA facilitating their maturation [25]. Since La uses two sites (LAM and RRM1) to produce high affinity binding of pre-tRNA, binding with one site alone results in lower target affinity and lower stability. Therefore, once a 3' trailer is cleaved La interacts with the mature tRNA and the 3'trailer both with lower affinity causing it to dissociate and recycle onto a new pre-tRNA whereby both of its binding sites can be utilized simultaneously [22]. As mentioned previously La is not essential to ensure viability in yeast, therefore a La-independent mechanism is present allowing for the proper processing of pre-tRNA. In the absence of La, the 3' trailer which is normally protected from 3' exonucleases is processed first by Rex1p. If the pre-tRNA contains the proper folding and is deemed functional by surveillance mechanisms within the nucleus, RNase P then removes the 5' leader and it is exported into the cytoplasm. Unfortunately, in this La-independent pathway, if the pre-tRNA is structurally impaired it becomes targeted for degradation by 3' exonucleases [25]. Interestingly, when La is overexpressed in yeast it is able to rescue misfolded and structurally impaired pre-tRNAs and allows for their processing and maturation into functional tRNAs [5].

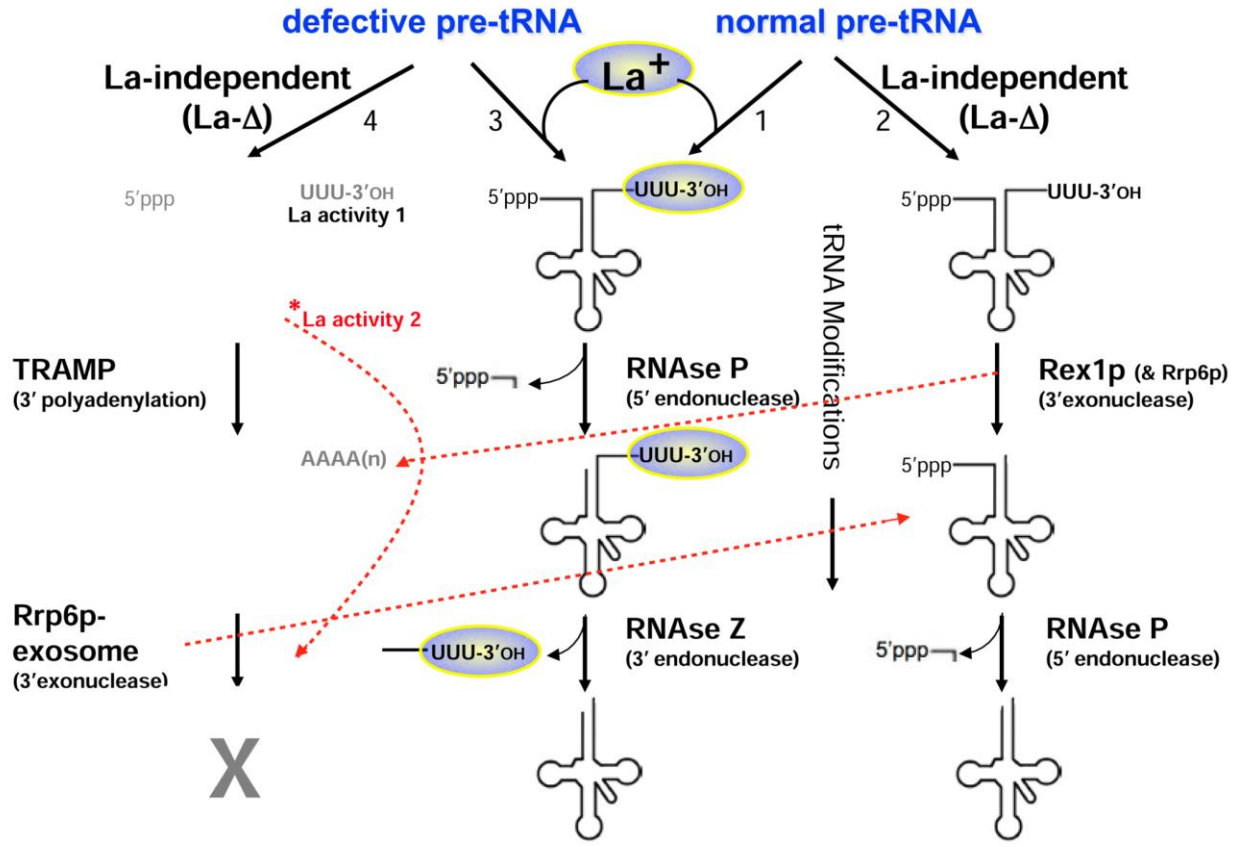

Figure 5: *La-dependant and La-independent pathways for pre-tRNA processing and maturation. The processing of pre-tRNAs can take one of four pathways. Normal and defective pre-tRNAs processed in a La-dependant manner (seen in the middle pathway) first have their 5' leader sequence cleaved by RNAse P followed by elimination of their 3' uridylate trailer by RNase Z. In the absence of La, the order of this processing is reversed with normal pre-tRNAs. (rightmost pathway) however, a functionally mature tRNA is still created. In contrary, defective pre-tRNAs can not be processed into a functional mature tRNA in the absence of La (pathway on the left) and therefore, are targeted for degradation by 3' exonucleases. Defective pre-tRNAs, when processed in a La-dependant manner result in functional mature tRNAs that can participate in protein translation. This highlights the importance of La's presence; it ensures initially defective pre-tRNAs are correctly processed to form functional tRNAs. Figure adapted from Bayfield et al. 2010* [25].

To further investigate La's role in tRNA processing, yeast strains containing a mutation that disrupts the secondary structure of essential tRNAs from forming were shown to be non-viable upon deletion of La [16, 23]. These structurally impaired pre-tRNAs were more susceptible to degradation from surveillance activities of the TRAMP polyadenylation complex which polyadenylates aberrantly formed RNAs targeting them to the nuclear exosome Rrp6 for removal. Furthermore, the absence of proper tRNA modifications can sensitize certain pre-tRNAs to degradation by the nuclear surveillance system. For example, in the case of pre-tRNA^{i} Met, failure to be methylated on adenine 58 by the tRNA methyltransferase TRM61 leads to the nuclear degradation of the hypomodified pre-tRNA. Overexpression of La can prevent the degradation of this pre-tRNA and permit the mature hypomodified tRNA^{i} Met to be exported into the cytoplasm where it functions appropriately in translation [24]. Such findings indicate a more complex mechanism is present in conjunction with the simple 3' end binding which enables La to rescue structurally impaired precursor tRNAs and hypomodified pre-tRNAs that would normally be targeted for destruction. The RNA binding domain responsible for this RNA chaperone activity has been localized to the RRM1 of human and *S. Pombe* La proteins [20, 22].

1.5 La Related Proteins: LARPs

La related proteins commonly referred to as LARPs are a collection of proteins which contain a conserved 90 amino acid signature La motif similar to that of the genuine La protein [33]. Humans carry five LARP subfamilies; LARP1 with variants 1a and 1b, LARP3, LARP 4 with variants 4a and 4b, LARP6 and LARP7. The genuine La protein has recently been termed as LARP3 by the HUGO gene classification system, but will continually be referred to as La or genuine La protein for the duration of this thesis.

Although two variants of LARP1 exist and contain about 60% homology with one another, all published work to date has been completed on the more abundantly processed LARP1a which provides a stronger knockdown phenotype [34]. Unlike genuine La protein which is normally located in the nucleus, LARP1 is predominantly cytoplasmic. LARP1 was the first of the LARP family shown to bind with PABP in an RNA-independent manner [35]. Knockdown of LARP1 is associated with a 15% reduction in overall protein synthesis and an increase in hypophosphorylated 4E-BP1, implying its involvement with cap-mediated mRNA translation [34]. Despite all of this, LARP1 contains all of the conserved amino acids with in its La motif required for 3' UUU-OH recognition.

To date there are two known paralogues of LARP4 identified as LARP4a and LARP4b. These LARP4 variants are the most divergent subfamily of LARPs from the genuine La protein. They lack key aromatic and basic side chain residues with in the La motif required from 3' terminal uridylate sequence recognition suggesting that they may have distinct RNA targets they engage with [25]. LARP4a is found with in the cytoplasm of

cells where it stimulates mRNA translation in part through the scaffold protein Ribosome-associated receptor for activated C kinase (RACK1) with cytosolic PABP and mRNAs via their polyadenylate tails [36]. LARP4b, previously termed as LARP5 only shares 34% homology overall with LARP4a but 74% homology between their La modules. LARP4b is predominantly found in the cytoplasm where it has been shown to stimulate translation and co-sediment with the 40s ribosome component either directly, or through its interaction with RACK1 [37].

LARP6 contains a conserved La module that can recognize 3' UUU-OH sequences as well as a uniquely conserved SUZ-C motif at it's C terminus believed to contribute to mRNA substrate recognition [38]. Mammalian LARP6 has been shown to interact with developmental transcription factor Cask-C [39,40] and functions upstream of transcription factor MyoD to control muscle development [39,40,41]. In addition to a transcription factor-associated protein LARP6 has been shown to specifically bind to a conserved stem-loop motif in the 5'UTR of α1 collagen mRNAs [42]. Thus, LARP6 shuttles between the nucleus and cytoplasm while participating in the nuclear export of collagen mRNAs [43].

LARP7 is an RNA binding protein with high homology to the genuine La protein in it's La module however, it does contain a divergent c-terminal domain. Like the genuine La protein, LARP7 binds to pol III transcripts but replaces La protein by specifically recognizing the 3' UUU-OH of a single RNA pol III transcript the 7SK snRNA [44]. 7SK snRNA is an abundant non-coding RNA that regulates mRNA metabolism by controlling the activity of the positive transcription elongation factor b (P-TEFb) [45] a

kinase required for RNA pol II transcription elongation. Because of this, like genuine La protein, LARP7 primarily resides in the nucleus of cells.

1.6 La's NRE can modulate its intracellular localization

The Nuclear retention element located in La's divergent C terminal domain is found between amino acids 316-332.This region has been shown to play an important role in controlling La's intracellular localization. Studies have shown that La without its NRE (ΔNRE mutants) clearly illustrates cytoplasmic localization compared to wild-type La which remains almost entirely nuclear (Figure 6) [30]. To clarify whether removal of the NRE causes inappropriate export from the nucleus or non-functional import into the nucleus, cells expressing hLa-ΔNRE were treated with leptomycin-B (LMB). LMB is responsible for blocking CRM1 mediated export from the nucleus. Therefore, RNAs recognized by hLa for proper processing and CRM1 for export, would be denied access out of the nucleus [31, 13]. Blocking CRM1 export resulted in substantial restoration of ΔNRE mutants into the nucleus confirming that the absence of the NRE results in the inappropriate export of La. This is distinct from La mutants which have their NLS deleted (hLa 1-375). Although these mutants contain a cytoplasmic phenotype, LMB treatment has no restorative effect indicating the non-functional import of these mutants into the nucleus. Furthermore, yeast expressing ΔNRE mutants show an accumulation of aberrantly processed tRNAs. Due to the inappropriate export of ΔNRE mutants into the cytoplasm, the tRNAs associated with them do not have their 5' leader or 3'trailer removed thus resulting in spliced tRNAs with unprocessed ends [30]. These aberrantly

processed tRNAs have lost their functionality required for protein translation [8]. LMB treatment restored the proper pre-tRNA processing in yeast containing ΔNRE mutants therefore concluding that the NRE is not responsible in La's pre-tRNA processing activities, instead, its presence is simply required to keep La nuclear in order for the proper processing of 5' and 3' ends to occur. Attempts to decipher the determinants within the NRE that cause its cytoplasmic phenotype lead to the discovery of two conserved lysine residue found at positions 316 and 317 in La. Mutations made to these lysine residues converting them into alanine (KK mutants) resulted in the same inappropriate export that was seen with the ΔNRE mutants. These KK mutants also generated aberrantly processed non-functional tRNAs [8] indicating the importance of lysine residues 316 and 317 in controlling NRE's intracellular trafficking of La. Interestingly, compensatory mutations made to the RRM1 of ΔNRE mutants restore nuclear localization and pre-tRNA processing, these double mutants include: ΔNRE E132A D133A and ΔNRE F150A.

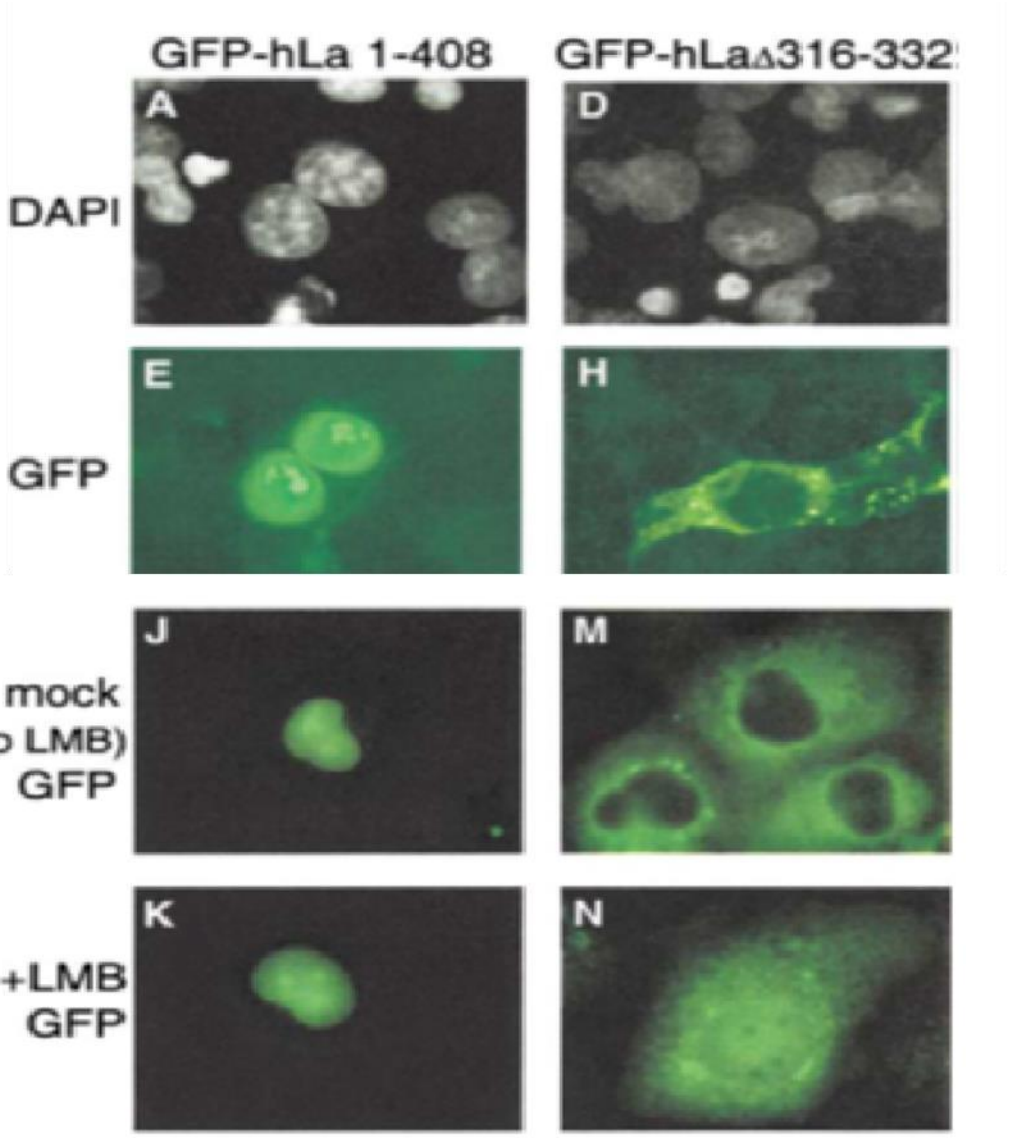

Figure 6: *Intracellular localization of GFP tagged hLa (right) and GFP tagged hLa-ΔNRE. Under normal conditions, fluorescence emittance from the tagged protein shows that hLa is nuclear (E) while hLa-ΔNRE mutants are exported to the cytoplasm (H). Blocking all crm1 mediated export from the nucleus through treatment of cels with leptomycin b (LMB) results in nuclear accumulation of hLa-ΔNRE mutants (N). LMB treatment on cells expressing GFP-hLa yields no change in intracellular localization. Adapted from Intine et al. 2002* [30].

1.7 Thesis Proposal

To date, no model or regarded mechanism has been generated to explain the cytoplasmic phenotype associated with hLa-ΔNRE mutants. This thesis will attempt to improve our understanding into what makes hLa's NRE so important for maintaining its nuclear phenotype and why the protein becomes cytoplasmic when its mutated or removed. Based on the complexity of hLa's RNA binding modes and the variety of RNA targets it binds to, we hypothesized that the inappropriate nuclear export of hLa- ΔNRE may be an indirect consequence of altered RNA target binding in cells. More specifically, we hypothesize that the NRE is important for maintaining hLa's appropriate conformation for binding precursor tRNAs substrates in the nucleus; with its removal making the protein more vulnerable to binding less favoured RNA substrates. This defect in RNA substrate specificity could make ΔNRE mutants more vulnerable to inappropriate export from the nucleus.

To investigate target RNA binding differences, EMSAs were used to compare the interaction between hLa and ΔNRE mutants with U10 and A20 RNA oligomers as well as with CGC alanine pre-tRNA substrates. The U10 oligomer was used to examine any affinity differences in La's 3' terminal uridylate binding mode whereas the A20 oligo was selected to identify any differences in the protein's poly A binding mode. Furthermore, CGC ala pre-tRNA was used to examine any differences in binding affinity with La's most characterized binding substrate: precursor tRNAs. ΔNRE mutants containing additional compensatory mutations in the RRM1 domain (E132A D133A or F150A) that were shown to restore nuclear localization [8] were also tested against the same RNA

substrates to pinpoint any binding similarities shared with hLa that could explain their similar cellular localization phenotypes. In addition to this, recent unpublished hydrogen-deuterium exchange (H/D exchange) mass spectrometry data from a collaborating lab has emerged identifying a potential inter-protein domain salt bridge interaction. The glutamate and aspartate residues at positions 132 and 133 in La's RRM1 and the lysine residues at 316 317 in the NRE could be critical in La's ability to discriminate between various RNA targets. We decided to take advantage of the ΔNRE mimicking phenotype of the previously mentioned "KK mutant" with a slight alteration. Instead of inserting alanine residues at positions 316 and 317 to disrupt this proposed salt bridge interaction, negatively charged glutamic acid residues were used. Substitution with glutamate residues instead of alanine allows us to potentially restore this salt bridge (and hopefully wildtype hLa activity) by inserting lysine residues at positions 132 and 133 creating a hLa E132K D133K K316E K317E mutant. This mutant's interaction with the aforementioned RNA substrates was also examined using EMSAs.

Next, we wanted to examine how hLa, hLa-ΔNRE and the various point mutants behaved when simultaneously presented with the opportunity to bind two different RNA targets. Thus, competition EMSA analysis were conducted to investigate this. A constant amount of radioactively labelled pre-tRNA was incubated with increasing amounts of cold (non-radioactive) A20 oligomer to see whether this increase in cold A20 would sufficiently compete off pre-tRNAs for binding. Identifying how hLa, ΔNRE and point mutants behave upon simultaneous exposure to multiple RNA targets may uncover a mechanism by which to explain La's cellular localization phenotype.

Finally, we sought to identify the relative proportion of tRNA and mRNA sequences interacting with hLa and hLa-ΔNRE in vivo. Being strictly nuclear, and involved with pretRNA processing, it was proposed that hLa would bind to a greater proportion of tRNAs in comparison with mRNA targets. Conversely, it was hypothesized that ΔNRE mutants might interact more so with mRNA targets due to its cytoplasmic phenotype and lower affinity pre-tRNA binding. To check for this, Hek 293T cells were transfected with GFP tagged hLa and ΔNRE mutants. The RNA targets interacting with these proteins where pulled down using cross-linking immunoprecipitation (CLIP) and subsequently subjected to northern blot analysis using probes that recognize methionine tRNA and Poly A sequences. Quantification of these northern blots would enable us to calculate a ratio of tRNA to mRNA sequences immunoprecipitated with hLa and the cytoplasmic hLa-ΔNRE mutant. The goal from this is to then see if these results support the RNA target binding affinities obtained from the in vitro EMSA data.

MATERIALS AND METHODS

2.1 Site directed Mutagenesis

To create the hLa-ΔNRE double mutant ΔNRE E132A D133A, the salt bridge disrupting hLa K316E K317E mutant and the salt bridge restoring hLa E132K D133K K316E K317E mutant site directed mutagenesis was conducted. The forward and reverse oligo primers (IDT Technologies) containing the appropriate point mutations to create the desired amino acid conversions for each protein are summarized in Table 1.

***Table 1**: Primer sequences used for site directed mutagensis of hLa pet28A and hLa-ΔNRE pet28A vectors.*

Primer name	Primer sequence
hLa E132A D133A For	5'-ACTCTTGATGACATAAAAGAATGGTTAGCAGCTAAAG GTCAAGTACTAAATATTCAGATG-3'
hLa E132A D133A Rev	5'-CATCTGAATATTTAGTACTTGACCTTTAGCTGCTAACCATT CTTTTATGTCATCAAGAGT-3'
hLa E132K D133K For	5'-CTCTTGATGACATAAAAGAATGGTTAAAAAAGAAAGGTCAAGTACT AAATATTCAGATG-3'
hLa E132K D133K Rev	5'-CATCTGAATATTTAGTACTTGACCTTTCTTTTTTAACCATTCT TTTATGTCATCAAGAG-3'
hLa K316E K317E For	5'-GAAGGAGAGGTGGAAAAAGAAGCACTGGAGGAAAT AATAGAAGACCAACAAGAATCCC-3'
hLa K316E K317E Rev	5'-GGGATTCTTGTTGGTCTTCTATTATTTCCTCCAGTGCT TCTTTTTCCACCTCTCCTTC-3'

The forward and reverse primers for E132A D133A, K316E K317E and E132K and D133K were diluted to create a 200μM stocks. The “Quick-change” procedure used to perform the site directed mutagenesis was performed in a 50μL reaction summarized in table 2.

Table 2: *PCR setup used for site directed mutagenesis of hLa pet28A and hLa-ΔNRE pet28A vectors.*

COMPONENTS	FINAL CONCENTRATION	VOLUME (μL)
5x Reaction Buffer	1X	10
10mM dNTPs	0.2mM	1
20μM Forward Primer	0.5μM	1.25
20μM Reverse Primer	0.5μM	1.25
Mini-Prepped DNA	0.5-0.7μM	1
Phusion Enzyme	1 unit/50μL PCR reaction	1
RNase Free water		35
Total		50

Table 3: *PCR cycle settings for site directed mutagenesis of hLa pet28A and hLa-ΔNRE pet28A vectors.*

CYCLE STEP	TEMPERATURE	DURATION	NUMBER OF CYCLES
Lid	105°C		
Initial Denaturation	98°C	6 min	1
Denaturing	98°C	30 sec	20
Primer Annealing	50°C	30 sec	
Extension	72°C	16 min	
Final Extension	72°C	16 min	1
Hold	4°C		

The 6 hour procedure was then held at 4 ^{o}C overnight. Reaction samples were then treated with 1µL of Dpn I (N.E Biolabs cat #: R0176S) and placed in the 37^{o}C water bath for 1 hour to eliminate the methylated parental vector. The Dpn I treated samples were then placed in 65^{o}C water bath for 15 minutes to denature the Dpn I enzyme.

2.1.1 Transformation of double mutants into *E.Coli* XL-1 strain

The hLa and ΔNRE pet28A plasmids mutated via site directed mutagenesis were transformed into *Escherichia Coli* XL-1 gold strain and plated on kanamycin plates to check for bacterial colony formation. As a positive control to ensure that hLa and ΔNRE pet28A mini-preps yielded enough template required for mutagenesis, these non-mutated mini-preps were also transformed into XL-1 to check for colony formation. The

bacterial transformations were performed as follows; 4µL of quick-change product was added to 50µL of thawed XL-1 gold cells in a pre-chilled microfuge tube and left to incubate on ice for 20 minutes. For mini-prepped samples, 1µL of ΔNRE pet28A vector (26.4ng) and hLa pet28A vector (34.6ng**)** were added to 25µL of XL-1 gold cells and incubated on ice for 20 minutes. Samples were heat shocked in a 37^{o}C water bath for 90 seconds to allow the vector DNA to enter bacterial cells. After heat shocking, samples were placed on ice for 2 minutes. Addition of LB media to the heat shocked samples was performed by a bunsen burner flame to ensure a sterile setting. For mutated hLa and ΔNRE vectors 400µL of media was added while mini-prepped samples containing fewer cells (25µL) were given 200µL of media. Samples were placed in a 37^{o}C water bath to incubate for 70 minutes. Because the pet28A vector contains kanamycin resistance, plating on LB kanamycin plates acts as a selection method for growth of only XL-1 cells transformed with the appropriate hLa or ΔNRE pet28A vector. Plating was performed in a sterile setting using a bunsen burner, the entire quantity of the samples (225µL of transformed cells containing the mini-prepped vector and 450µL containing the mutated vector) were added to the plate. To ensure even distribution of the XL-1 cells within the plate, 10-15 sterile beads were added and shaken inside the plate. Beads were discarded, and the plates were placed upside down in the 37^{o}C incubator overnight. Colonies formed on the plates containing the transformed hLa and ΔNRE mutants were picked and added to round bottom conical tubes containing 5mL of LB media and 25µL of kanamycin (10mg/mL) in the presence of a flame. These cultures were grown overnight in a 37^{o}C shaker (Eppendorf innova 40) at 200 RPM.

2.1.2 Mini-prep of *Escherichia coli* XL-1 strains

Overnight XL-1 bacterial cultures transformed with mutated variants of hLa and ΔNRE pet28A vectors were mini-prepped in order to obtain DNA. The Omega Bio-Tek E.Z.N.A plasmid mini DNA kit I quick guide centrifugation protocol was used to perform all mini preps completed in this thesis. The presence of E132A D133A point mutations in the ΔNRE pet28A vector along with the E132K D133K and K316E K317E point mutations in hLa pet28A were confirmed through sequencing services provided by the Hospital for Sick Children (TCAG sequencing Facility).

2.2 Protein Expression and Purification

2.2.1 LB Media Preparation

In order to support bacterial cells growth and expression of protein, 1 LB cultures were prepared with the following recipe: 10g NaCl (Multipharm cat #: K35163700 539), 10g Peptone (Fisher Scientific cat #: 73049-73-7) and 5g of yeast extract (Bioshop cat #: 8013-01-2). After thorough mixing with a magnetic stirring rod at 1000RPM for 5 minutes, media was autoclaved.

2.2.2 Seeding LB Culture and Protein Induction

Two overnight cultures were seeded into 1L of LB media that was pre-heated in a 37^{o}C shaker (Eppendorf innova 43) for 15 minutes. To prevent contamination, 5mL of kanamycin was added for a final concentration of 0.05mg/mL. After seeding down, the 1L cultures were left to grow for 3 hours at 37^{o}C at 200RPM until an O.D 600 reading of 0.6-1.0 (mid-log) was achieved. Using proper sterile technique, 1mM of IPTG (Fisher Scientific cat #: 367-93-1) was added to the 1L cultures to induce protein expression for 3 hours. After 3 hours of protein induction, the 1L cultures were transferred to 1mL Beckman centrifuge bottles. Cells were pelleted at 6000 RPM for 15 minutes at 4^{o}C using the Beckman Avanti J 9.1 rotor. The supernatant was removed and the pellet was re-suspended into a 50mL conical tube using of a pellet transferring buffer consisting of 2.5mL of 1M Tris pH 7.4 and 0.29g NaCl in 50mL of dH_20. The broth was then spun in a centrifuge (Eppendorf 5430R) using a F-35-6-30 rotor at 6000 RPM for 15 minutes at 4^{o}C. The supernatant was removed, and the pelleted cells were stored in a -80^{o}C freezer.

2.2.3 Protein Purification Using His-trap Columns

Recombinant proteins containing a 6x His-tag on their C-terminal domain were purified using Ni^{2+} affinity chromatography. Cell pellets stored from protein induction were thawed on ice and re-suspended in 10 mL of lysis/binding buffer (50mM Tris HCl pH 7.6, 500mM NaCl, 0.05% Igepal, 20mM Imidazole, 5mM β-mercaptoethanol). Following re-suspension, 100µL of protease inhibitor cocktail (Sigma Cat #: P8849) was added. To disrupt the cell membranes, cells were sonicated (Misonix XL-2000 series) in pulses lasting 15 seconds at 0.05W followed by a 15 second break period for a total of 12 minutes. The sonicated samples were spun at max speed for 30 minutes at 4°C in the Eppendorf 5430R centrifuge, and the supernatant was transferred into a 15mL conical tube. To ensure elimination of all cellular debris, a second spin at max speed for 20 minutes at 4°C was completed and the supernatant transferred to a new 15mL conical tube. For purification, a separate 1mL Ni^{2+} His-trap FF column (GE Healthcare Cat #: 17-5319-01) was used for each protein. Columns were first washed with 5mL of ddH_2O followed by 5mL of lysis binding buffer to equilibrate the columns. Next, 10mL of lysate was added to the column using a sterile 15mL syringe. The flow-through was collected in a 15mL conical tube and stored for SDS-PAGE analysis. Columns were then washed 3 times with 5mL of wash buffer (50mM Tris HCl pH 7.6, 500mM NaCl, 20mM Imidazole, 1mM β-mercaptoethanol) with each wash collected in a separate 15mL conical tube for SDS-Page. Finally, 5mL of elution buffer (50mM Tris HCl pH 7.6, 500mM NaCl, 300mM Imidazole, 5mM β-mercaptoethanol,1 mM EDTA) was ran through the column and collected into a 15mL conical tube.

2.2.4 Protein Cleaning Using HiTrap Heparin HP Columns

Heparin columns were used to eliminate any residual nucleic acids that may still be bound to the protein after purification. The 5mL protein elution obtained from the final step of the His-trap purification was loaded into a 1mL HiTrap Heparin HP column (GE Healthcare Cat #: 17-0406-01) using a sterile 15mL syringe. The flow-through was collected in a 15mL conical tube and stored for SDS-Page analysis. Heparin columns were then washed with 5mL of 1X EMSA buffer (20mM Tris-HCl PH 7.6, 100mM KCl, 0.2mM EDTA, 1mM DTT) and collected into a 15mL conical tube. Subsequent 5mL washes were conducted using 1X EMSA buffer containing increasing amounts of KCl to displace the protein off the column. These washes consisted of final KCl concentrations of 200mM, 400mM, 800mM, 1.2M and 2M. All washes were collected in 15mL conical tubes for SDS-page. After KCl washes, columns were rinsed with 10mL of ddH_2O followed by 5mL of 20% ethanol and stored at 4^oC. The 800mM KCl washes were then desalted to remove excess imidazole and KCl present in the buffer. A 1:1 ratio of protein elution and chaperone buffer (50mM Tris HCl pH 7.6, 1mM DTT, 1.5mM $MgCl_2$) were added to 5mL concentrator tubes (Amicon Ultra, 10 kDa) and spun at 5000 RPM for 40 minutes at 4°C. Flow through from the concentrator column was discarded and additional chaperone buffer was added for a final volume of 4 mL. The samples were spun down to a final volume of 100-150µL as indicated by the scale on the concentrator column. Glycerol was added for a final concentration of 5% and samples were stored at -80^oC.

2.3 RNA labelling with ^{32}P ATP

2.3.1 A20, U20 and U10 Labelling with γ-^{32}P ATP

To label the 5'end of RNA, T4 polynucleotide kinase (PNK) was used to transfer the γ-^{32}P of the ATP (PerkinElmer) to the 5' end of the A20, U20 and U10 oligos (IDT). The labelling reaction for each substrate was completed in a 20µL final volume using the following setup: 2µL of 20µM oligo RNA, 2µL of γ-32ATP (activity of 3000Ci/mmol), 2µL of 10X T4 PNK buffer, 1µL T4 PNK, 13µL RNase free H_2O. The samples were incubated at 37°C for 2 hours to allow for sufficient labelling of the RNA oligos.

2.3.2 Labelling CGC precursor tRNA with α-^{32}P ATP

CGC alanine pre-tRNA was radioactively labelled with α-^{32}P ATP using an Sp6 promoter transcription Kit (Ambion MEGAscript SP6 Cat#: AM 1330). This ATP with a radioactively labelled phosphate at the α position becomes incorporated into the pre-tRNA sequence during transcription making it radioactive. The Sp6 reaction was completed in a 20µL final volume with the following setup: 2µL of 75mM CTP, UTP and GTP. 2µL of 0.75mM ATP, 2µL of reaction buffer, 125nM of CGC pre-tRNA template, 2µL of α-^{32}P ATP (activity of 3000Ci/mmol), 2µL Sp6 polymerase and 4µL of DNase RNase free H_2O. The sample was then placed at 37°C overnight.

2.3.3 Gel Extraction of ^{32}P Labelled RNA

After RNA labelling, 5µL of formamide dye (80% deionized formamide, 10 mM EDTA, 0.06% bromophenol blue, 0.06% xylene cyanol) was added and samples were heated at 95°C for 8 minutes. The A20, U20 and U10 samples were then loaded on a 15% denaturing urea gel whereas CGC pre-tRNA samples were loaded onto a 10% urea gel (1X TBE, 15% or 10% polyacrylamide, 7M urea, 0.08% APS, 0.037% TEMED). Gels were run at 100V at 4°C with 1X TBE as the running buffer until the bromophenol blue dye reached ¾ the length of the gel. The gel plates were opened and the exposed side was placed facing upwards in a cassette. Plastic wrap was used to cover the exposed side and Glogos ® II Autoradmarkers (Agilent technologies Cat#: 420201) were placed on each side of the gel as markers for band location. In a dark room, HyBlot CL Autoradiography film (Denville Scientifc Cat#: E3012) was placed on the gel for a 2 minutes. Films were developed showing the location of the radioactive bands within the gel. Using the developed film as a guide, the radioactive bands were extracted using a razor and placed in a 0.5 mL microfuge tube with the bottom of the tube cut off. This microfuge tube was placed in a 1.5mL microfuge tube and spun down for 1 minute at 14 000 RPM (Eppendorf 5415C) to shred the extracted gel into small pieces. The resulting pieces were then immersed in 250µL of 0.5M NaCl overnight to elute the RNA. A scintillation counter (Hidex 300SL) was used to determine the activity in CPM of the radioactive RNA (1µL of RNA in 7mL of scintillation fluid).

2.4 Electrophoretic mobility shift assay (EMSA)

To assess protein interaction with the various RNA substrates, electrophoretic mobility shift assays were conducted. 10X EMSA buffer (200mM Tris HCl pH 7.6, 50mM B-mercaptoethanol, 1M KCl, 10mM EDTA) was prepared for inclusion into master mix and for creation of the protein (La) dilution buffer. La dilution buffer (LDB) (1X EMSA, 10% glycerol in 200µL final volume) was used to dilute proteins varying from 0 – 8000nM. The exact amounts of buffers and radioactively labelled RNA added into the master mix was dependant on the number of lanes (1 gel = 10 lanes, 3 gels = 30 lanes etc;). The master mixes were set up as follows: 1X EMSA buffer/Lane, 10% glycerol/Lane, labeled RNA with an activity of 3000 cpm/lane, 10µL of bromophenol blue dye (diluted in RNase free water), and RNase free water for a final volume of 20µL multiplied by the number of lanes prepared. The master mixes were heated at 95°C for 4 minutes and then slow cooled back to room temperature. 2µL of protein diluted to 10X the required amount of was added to 18µL of master mix to create 1X final concentrations varying from 25-8000nM. A reaction with no protein (2µL of LDB buffer with 18µL of master mix) was used as a control lane representing 0nM of protein present. The reaction mixes were incubated at 37°C for 20 minutes, and then placed on ice for 5 minutes. A 6% native gel (1X TBE, 6% polyacrylamide, 0.08% APS, 0.037% TEMED) was pre-run for 15 minutes at 4°C with 1X TBE buffer. Samples were loaded and the gel was run at 100V at 4°C until the bromophenol blue dye ran ¾ of the way down the gel (for A20, U20 and U10) and entirely off the gel for CGC pre-tRNA. The gel was removed from the glass plates, placed on whatman filter paper (GE healthcare Cat

#: 3001-917) and then placed in a gel dryer (BioRad model 583) for 40 minutes at 80°C. Once the gels were dried, they were placed in an autoradiography cassette and left to expose on a storage phosphor-screen overnight. The screen was then scanned using a phosphor-imager (GE typhoon scanner) to visualize the radioactive protein-RNA complexes on the gel. The bands were quantified using the Image Quant TL software. These quantifications were implemented into Graphpad prism software to generate binding curves.

2.4.1 Competition EMSA

Identical setup as a standard EMSA with the following modifications. 1.) A Constant amount of protein (2µM final) used in each lane rather then an increase in concentration. 2.) 10X stocks of cold competitor RNA were made (5, 20,80 and 320µM) 3.) Reactions were setup in the following order; 16µL of master mix added first followed by 2µL of a 10X cold competitor RNA and 2µL of 10X protein stock to create a 1X final.

Samples were then incubated at 37°C for 20 minutes whereby the standard EMSA protocol was used to complete the experiment.

2.5 Cross-linking Immunoprecipitation (CLIP) assay

2.5.1 Transfection of Hek 293T cells

To obtain a sufficient yield of Hek 293T cells for downstream experimental applications, two 15cm dishes of cells were used per vector resulting in eight 15cm dishes for the 4 different expression vectors. These eight 15cm dishes containing Hek 293T cells at 75% confluency were transfected with either 15µg of GFP-tagged hLa, ΔNRE, 1-375 or c-myc-tagged PABP. This was completed by adding 15µg of vector DNA with 1.5mL of opti-MEM media (Gibco Cat #:31985-070) in one set of 15mL conical tubes and 40µL of lipofectamine 2000 (Life technologies Cat #:11668-027) with 1.5mL of opti-MEM media into a second set of 15mL conical tubes. After a 5-minute incubation, contents from the first set of conical tubes were added to the second set containing the lipofectamine 2000 and incubated together for 15-minutes at room temperature. During this incubation, Hek 293T cells were washed once with 10mL of PBS (Multicell Cat #: 311-010) and refed with 12mL of fresh 10% FBS DMEM (Gibco Cat #:11965-092) media without antibiotics. The 3mL opti-MEM solution containing vector-lipofectamine complexes were added to the 15 cm dishes and left to incubate for 6 hours to allow for transfection of vector DNA into cells. After incubation, cells were refed with fresh media containing 2% Pen Strep (Gibco Cat #:15070063) antibiotic.

2.5.2 UV crosslinking and harvesting of Hek 293T cells

Transfected cells were washed twice with 10mL of PBS to remove cellular debris. Two PBS washed 15cm plates were then placed into a UV cross-linker (Spectrolinker XL-1500) on a tray of ice. Plates were exposed to 1000mJ/cm^2 of UV radiation to covalently link all nucleic acids residues in direct or close contact with amino acid protein domains. Cross-linked cells were then resuspended in 3mL of RIPA buffer (50mM Tris PH 7.4, 150mM NaCl, 1% NP40, 1% Sodium deoxycholate, 0.01% SDS, protease inhibitor 1:1000 final, supeRNase inhibitor 1:1000 final) and aliquoted into 1.5mL microfuge tubes. Tubes were spun down at 4°C at maximum speed for 2 minutes to pellet cells. The supernatant was removed and cell pellets were stored at -80°C until immunoprecipitation.

2.5.3 Protein G bead preparation

Magnetic protein G Dynabeads (Thermoscientific Cat #: 10003D) were used for immunoprecipitation of GFP and C-myc-tagged proteins. For each sample, 65µL of protein G Dynabeads were washed twice with 400µL of RIPA buffer. Beads were then resuspended in 150µL of RIPA buffer and incubated with 10µg of GFP (Abcam Cat #: ab1218) or C-myc antibody (Abcam Cat #: ab32). As a negative control, 10µg of a human IgG control antibody (Thermoscientific Cat #: 31154) was used. The bead-antibody solutions were left to rotate at room temperature for 60 minutes to allow for the

interaction between the respective antibodies and protein G beads to occur. Beads were then washed 3 times with RIPA buffer prior to immunoprecipitation.

2.5.4 Cell lysis and partial RNA digestion

Hek 293T cell pellets where thawed on ice and later resuspended in 150µL of RIPA buffer. Cells transfected with the same vector where then pooled together into a single 1.5mL microfuge tube. To eliminate nucleic acid residues not bound to protein, 15µL of RNase I (Ambion Cat#: AM2295) diluted to 1:500 along will 2µL of turbo DNase (Ambion Cat#: 1340) were added to the resuspended cells. Samples were placed in a 37°C shaker for 4 minutes before immediately transferring them back onto ice. These samples were then spun at max speed (Eppendorf 5430R) for 45 minutes at 4°C and the supernatant collected for immunoprecipitation. Note: 10µL of this lysate was collected for western blot analysis to ensure efficient transfection of the vectors expressing GFP and C-myc tagged proteins.

2.5.5 Immunoprecipitation of GFP and C-myc tagged proteins

The cell lysate for each sample obtained from the previous step was equally distributed into two parts. The first half was added to beads containing control IgG antibody while the second half was added to the beads containing their respective antibody (GFP for hLa, ΔNRE, 1-375 and C-myc for PABP). The beads were left to rotate with the cell lysate for 2 hours at 4°C. After 4°C incubation, supernatant was

discarded and the beads were washed twice with high salt RIPA buffer (500mM of NaCl instead of 150mM) and twice with Proteinase K (PNK) wash buffer (100mM Tris PH 7.6, 500mM NaCl, 10mM EDTA). Prior to PNK treatment, 10µL of each sample was stored for western blot analysis to examine immunoprecipitation efficiency of GFP and C-myc tagged proteins. To remove all protein present in the IP samples, 200µL of PNK buffer along with 10µL of PNK were added and samples were placed at 37°C to incubate for 20 minutes. After incubation, 200µL of PNK urea buffer (PNK buffer + 0.7M urea) was added to each sample along with 10µL of PNK and incubated at 37°C for 20 minutes. To extract the immunoprecipitated RNA for northern blot analysis, 400µL of acid phenol (Sigma Cat #:) was added to each sample and vortexed for 5 seconds to mix thoroughly. Samples were then spun at max speed for 10 minutes at 4°C. The top aqueous layer was collected into a new microfuge tube where 400µL of chloroform (Bioshop Cat #:) was added. Samples were spun at max speed for 10 minutes at 4°C. The top aqueous layer was collected into a new microfuge tube and precipitated by adding 1/10th the aqueous layer volume of 3M sodium acetate (ie: 40µL for 400µL of aqueous layer), 2.5 times aqueous layer volume with 100% etOH and 2µL of glycogen or glycoblue to aid in RNA pellet visualization. Samples were stored at -20°C over night.

2.5.6 Northern blot analysis of immunoprecipitated RNA

Precipitated RNA samples were spun down for 10 minutes at max speed at 4°C. The 100% ethanol was removed and the pellets were washed by adding 70% ethanol and spinning again at maximum speed for 10 minutes at 4°C. The 70% ethanol was

removed and the RNA pellets were left to air dry at room temperature for 4 minutes. The RNA pellets were then resuspended in 10µL of formamide dye and heated at 95°C for 10 minutes. In order to determine the size of bands seen on our membrane, 2µL of a radioactively labelled decade marker (Ambion Cat #: AM7778) was also mixed with 10µL of formamide dye and heated at 95°C for 10 minutes. Note: this marker was radioactively labeled using γ-^{32}P ATP following the protocol in 2.3.1 and gel extracted via 2.3.3. During this incubation a pre-made 12% urea gel was set up and allowed to pre-run for 20 minutes at 100V at 4°C. Prior to loading, any urea buildup with in the wells due to pre-running were cleared. The gel was left to run at 100V at 4°C for ~2 hours or until the bromophenol blue dye ran off the gel. After gel electrophoresis was completed, the samples were transferred onto a gene screen membrane (Perkin Elmer Cat #: NEF 1017001 PK) for northern blot analysis using the Invitrogen iBlot transfer system (Invitrogen Cat #: IB301002). After the 6-minute transfer, the membrane was crosslinked for 90 seconds (Fotodyne DNA transfer lamp) followed by drying for 10 minutes at 80°C (BioRad model 583). The membrane was then incubated for 2 hours with pre-hybe buffer (6X SSC, 2X Denhardt's solution (Thermo Scientific Cat #: 750018), 1% SDS, 200µL of total yeast RNA 10mg/mL (Thermo Scientific Cat #: AM7118), 20 mL final volume) in a rotating hybridization oven (Tek Star Jr). Note: If probing with dt40, the temperature was set to 32°C however, if probing with human Met tRNA the temperature was set to 37°C. The probe (radioactively labelled using the protocol from 2.3.1) was heated at 95°C for 5 minutes before being adding to the membrane submerged in the pre-hybe buffer. Hybridization of the labelled probe to the membrane was allowed to proceed overnight in a rotating hybridization oven. The next

morning, northern blots were washed 3 times for 20 minutes with wash buffer (2X SSC, 0.1% SDS) and then placed into an autoradiography cassette and left to expose on a storage phosphor-screen overnight. The screen was then scanned using a phosphor-imager (GE typhoon scanner) to visualize the radioactive probe. For sequential probing the membrane was stripped (0.1X SSC, 0.1% SDS) 3 times for 20 minutes at 70°C. Repeat methodology from pre-hybridization step to examine hybridization with additional probes.

2.5.7 Western blot analysis to check for transfection and immunoprecipitation efficiency

The 10µL of cell lysate obtained in 2.5.4 and immunoprecipitated samples in 2.5.5 were subject to western blot analysis to examine transfection efficiency of GFP and C-myc expressing vectors in Hek 293T cells as well as their respective Immunoprecipitation efficiency from anti-GFP and anti-C-myc linked protein G beads. Samples were mixed with 3µL of loading dye (30µL of 5x Laemmli, 3µL 2-beta mercaptoethanol) and heated at 95°C for 8 minutes before being loaded onto a 10% SDS PAGE gel. Transfection and IP samples were run at room temperature for 90 minutes at 125V. After SDS-PAGE, samples were transferred for 90 minutes at 50V onto a nitrocellulose membrane using transfer buffer (25mM Tris base, 190mM glycine) as the running buffer. The membrane was ponceau stained afterwards to check for the successful transfer of proteins and blocked overnight at 4°C using blocking buffer (1X TBS, 0.1% Tween, 3% skim milk). After blocking, the membrane was washed 3 times using 1X TBST buffer (1X TBS, 0.1%Tween) for 10 minutes followed by incubation with

primary antibody (1X TBST + 1/5000 dilution of anti GFP and C-myc antibody.) for 1 hour. The membrane was then washed 3 times with 1X TBST for 10 minutes and incubated with secondary antibody (1X TBST + 1/2000 dilution of goat anti-mouse IgG) for 1 hour. After secondary, a final wash with 1X TBST was completed, followed by the incubation with ECL for 2 minutes (Thermo Scientific Cat #: 32106). The western blot was developed using autoradiography film to confirm the transfection of GFP and c-myc expressing vectors in Hek 293T cells as well as the successful immunoprecipitation of protein-RNA complexes with anti-GFP and anti-c-myc linked protein G beads.

2.6 Immunoprecipitation of GFP-tagged proteins for mass spectrometry analysis

2.6.1 Transfection of GFP-tagged proteins into Hek 293T cells

Hek 293T cells grown to 75% confluency were transfected with 12µg of empty GFP vector along with GFP vectors expressing hLa and hLa-ΔNRE. To obtain a sufficient yield of cells for downstream applications, two 15cm plates of cells were grown per sample. Transfection was completed by added 12µg of vector DNA to one set of 1.5mL microfuge tubes containing 400µL of 1X DMEM and 30µL of polyjet (Frogga bio Cat #: SL100688) to a second set of microfuge tubes containing the same amount of media. After a 2 minute incubation, contents from the second set of tubes were added to the first set of tubes containing media and vector DNA. To allow for polyjet-vector DNA complexes to form, the solutions were left to incubate at room

temperature for 15 minutes. During this incubation, cells were washed once with 10mL of pre-warmed PBS and refed with 14mL of fresh media (10% FBS, 1X DMEM). The polyjet-DNA containing solutions were then added to the 15cm dishes and left to incubate at 37°C. After 5 hours, cells were refed with fresh media containing pen strep (Gibco Cat #:15070063) antibiotic.

2.6.2 Protein G bead preparation

Magnetic protein G Dynabeads (Thermoscientific Cat #: 10003D) were used for the immunoprecipitation of GFP tagged hLa, hLa-ΔNRE and an empty GFP control. For each sample, 65µL of protein G Dynabeads were added to 500µL of PBS with 0.1% tween. Next, 6µg of GFP primary antibody (Abcam Cat #: ab1218) was added to each sample and left to rotate overnight at 4°C. Note: bead preparation must be completed the night before making cell lysate.

2.6.3 Cell Lysis and Immunoprecipitation

Transfected cells were washed twice with 10mL of PBS to remove cellular debris and resuspended in 3mL. These resuspended samples were transferred over to 1.5mL microfuge tubes and centrifuged at maximum speed for 2 minutes to pellet cells and discard PBS supernatant. Cell pellets were resuspended into 5 volumes of NP-40 lysis buffer (50mM Tris-HCl PH 7.6, 150mM NaCl, 0.5% NP-40, 2mM EDTA, 100mM NaF, 10X Protease inhibitor cocktail (100µL aliquot/ 5mL of buffer)) and vortexed for 30

seconds every 10 minutes for 40 minutes. Note: keep samples on ice whenever possible. After cell lysis, spin down samples at 4°C for 10 minutes at maximum speed. Collect the supernatant as protein lysate. Before adding your lysate to the prepared protein G beads, wash twice with 400µL of PBS. Add up to 1mL of protein lysate to the beads and rotate samples overnight at 4°C.

2.6.4 Protein elution and buffer exchange

After overnight incubation at 4°C, beads were washed once with 500µL of NP-40 lysis buffer and twice with 500µL of NP-40 free lysis buffer (ddH_2O replaces NP-40 in buffer). Elute Protein-protein complexes from the beads by adding 500µL of 0.5M NaOH to each sample, rotate at room temperature for 20 minutes. Spin samples down for 2 minutes at 6000 RPM to pellet beads and collect supernatant into a 5mL concentrator conical (Amicon Ultra, 10 kDa). Fill up the concentrator with 50µM ammonium bicarbonate and spin at 5000RPM for 20 minutes at 4°C. Discard the flow through obtained in the collecting tube and repeat the process by refilling the conical tube with 50µM ammonium bicarbonate and concentrating the sample down to ~100µL. Collect the buffer exchanged samples into a new 1.5mL microfuge tube and store at -80°C until mass spectrometry analysis.

RESULTS

3.1 Proteins and radioactively labelled RNAs selected for EMSA analysis

To investigate any observable differences between how hLa and the binding modes of its various mutated forms change in vitro, four RNA substrates were labelled using ^{32}P ATP for EMSA analysis. A U20 oligomer was first used to test for differences in hLa's terminal 3' UUU-OH binding mode however, it was later decided that a U10 oligomer more accurately addresses this. An A20 oligomer was used to examine differences in the poly-A binding mode and a CGC ala pre-tRNA was used to observe differences in the tRNA binding mode (which encompasses the 3'UUU-OH binding mode). hLa, hLa-ΔNRE and "double mutant" proteins were used for analysis. The "double mutant" ΔNRE E132A D133A contains a secondary mutation in the RRM1 along with the removal of the NRE that has been shown to restore nuclear localization. Along with these mutants, a pair of substitution mutants were created based on the salt bridge interaction that is hypothesized between the glutamate and aspartate residues at positions 132 and 133 of the RRM1 respectively and the lysine residues at positions 316 and 317 of the NRE. Substitution of these lysine residues to glutamate residues breaks this salt bridge interaction generating a mutant (hLa K316E K317E) that contains a similar cytoplasmic phenotype seen with the ΔNRE mutant. In an attempt to fix this salt bridge interaction, the glutamate and aspartate residues at positions 132 and 133 were changed to lysine residues with the hopes that this "swapped mutant" hLa E132K D133K K316E K317E would be able to restore the binding activity that more resembles

wildtype hLa. The diagram in Figure 7 shows the various mutants created for EMSA analysis.

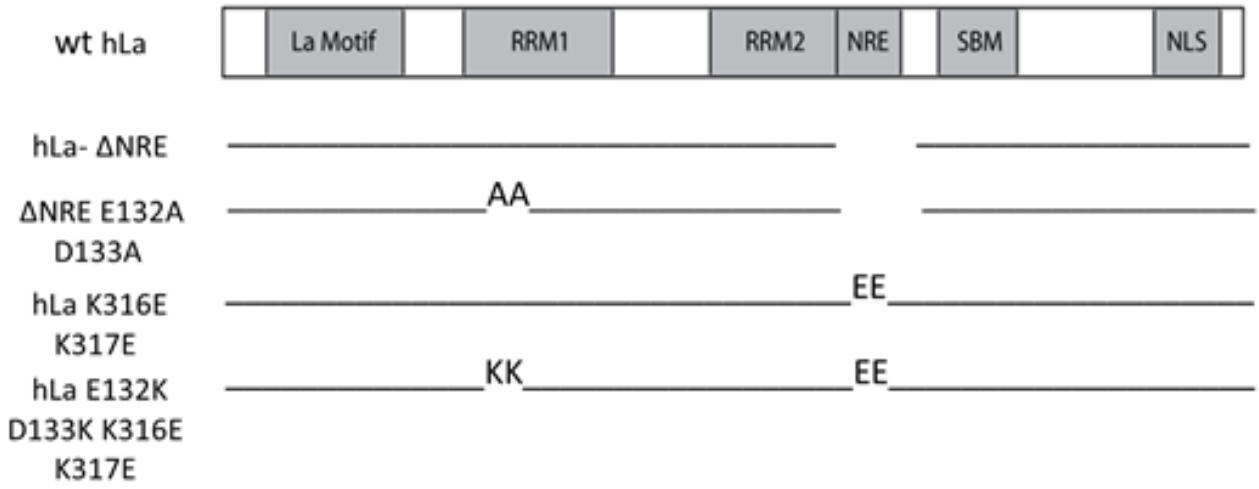

Figure 7: *The various proteins used for EMSA analysis. The double mutant ΔNRE E132A D133A not only lacks the NRE region, but contains additional substitution mutations in the RRM1 domain. hLa K316E K317E contains substitution mutations in the RRM1 while the hLa E132K D133K K316E K317E contains substitution mutations in both RRM1 and NRE*

3.2 ΔNRE and ΔNRE E132A D133A mutants show a reduction in affinity for U20 but not U10 binding upon comparison with hLa.

Figure 8 A-C displays the gel shift results for U20 binding with wildtype hLa, its ΔNRE mutant, and the ΔNRE E132A D133A double mutant. In comparison with wildtype (Kd: 220nM), the ΔNRE mutant exhibits a substantial reduction in its affinity for the poly U substrate (Kd: 620nM). Wildtype La shows initial binding to its U20 target at 250nM and complete binding by 500nM (8A). The ΔNRE mutant begins its binding at 500nM and achieves complete binding by 1000nM (8B). Quantification of these EMSAs were completed and binding curves created using prism (8D). The rightward shift seen by ΔNRE (blue line) in the binding curve confirms the drop in poly U affinity. The double mutant also shows a reduction in U20 affinity (Kd: 921nM) as seen by both the gel shift in 8C and the binding curve 8D. The issue with using a U20 oligomer to examine hLa's 3' UUU-OH binding mode is that this 20-mer of U's is sufficiently long enough to make additional contacts with the protein outside of the La module binding pocket known for binding these sequences. Therefore, the binding differences seen between hLa and ΔNRE mutants could mean: 1) an important role for NRE in 3' UUU-OH binding mode (which has not been shown in the literature to date) or 2) the U20 oligomer is making additional contacts with the CTD to strengthen its interaction with hLa that is not possible with ΔNRE mutants thus resulting in their differences of affinity.

To examine this, a U10 oligomer was used to test for 3’ UUU-OH dependant binding. This 10-mer is not long enough to make any additional contacts outside of the La module and therefore serves as a more accurate means of examining hLa’s terminal uridylate binding mode. Figure 9 A-C shows the EMSAs for hLa, ΔNRE and the ΔNRE E132A D133A double binding to the U10 oligo respectively. Using U10 as an RNA substrate instead of U20, the substantial differences in affinity originally seen between hLa and the ΔNRE mutants were eliminated (Kd values of 451nM and 676nM respectively). In addition, the nearly identical binding curves of all three proteins in figure 9D illustrates this no-change. Collectively these data suggest that the NRE plays no direct role in La’s 3’UUU-OH binding however; if poly U sequences are sufficiently long enough (greater then 10), they could potentially interact with this region increasing the protein’s affinity for this substrate.

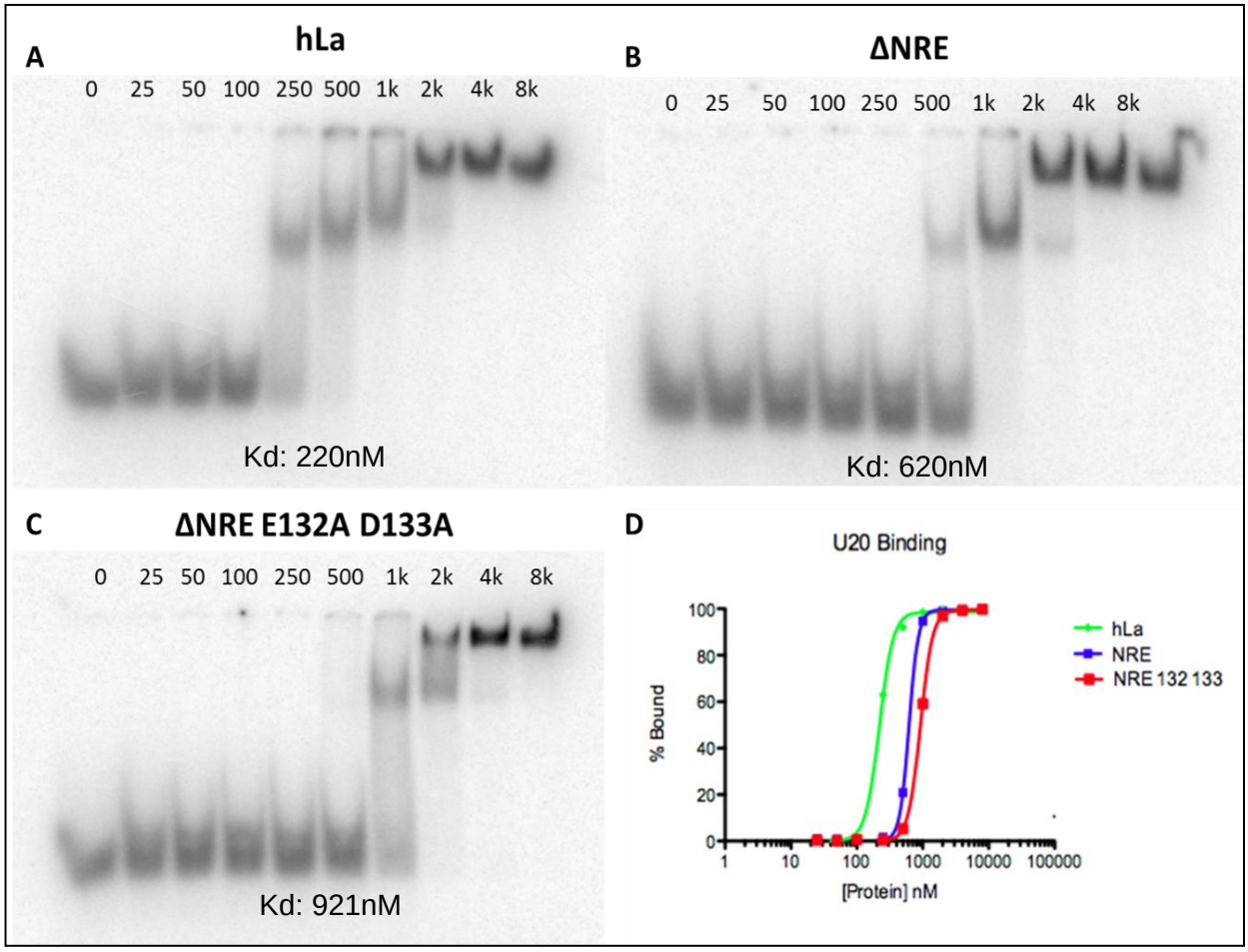

Figure 8: *(A-C) EMSA results displaying wild type hLa, hLa-ΔNRE and the ΔNRE E132A D133A double mutant binding with a radioactively labelled U20 substrate. A drop in affinity for the U20 oligomer is observed between wildtype (Kd: 220nM) and ΔNRE (Kd: 620nM) followed by a subsequent reduction when comparing wildtype hLa with the double mutant (Kd: 921nM). (D) Binding curve highlighting the percentage of bound protein over increasing concentrations. The rightward shifts associated with ΔNRE (blue) and double mutants (red) illustrate their drop in affinity for the U20 oligomer.*

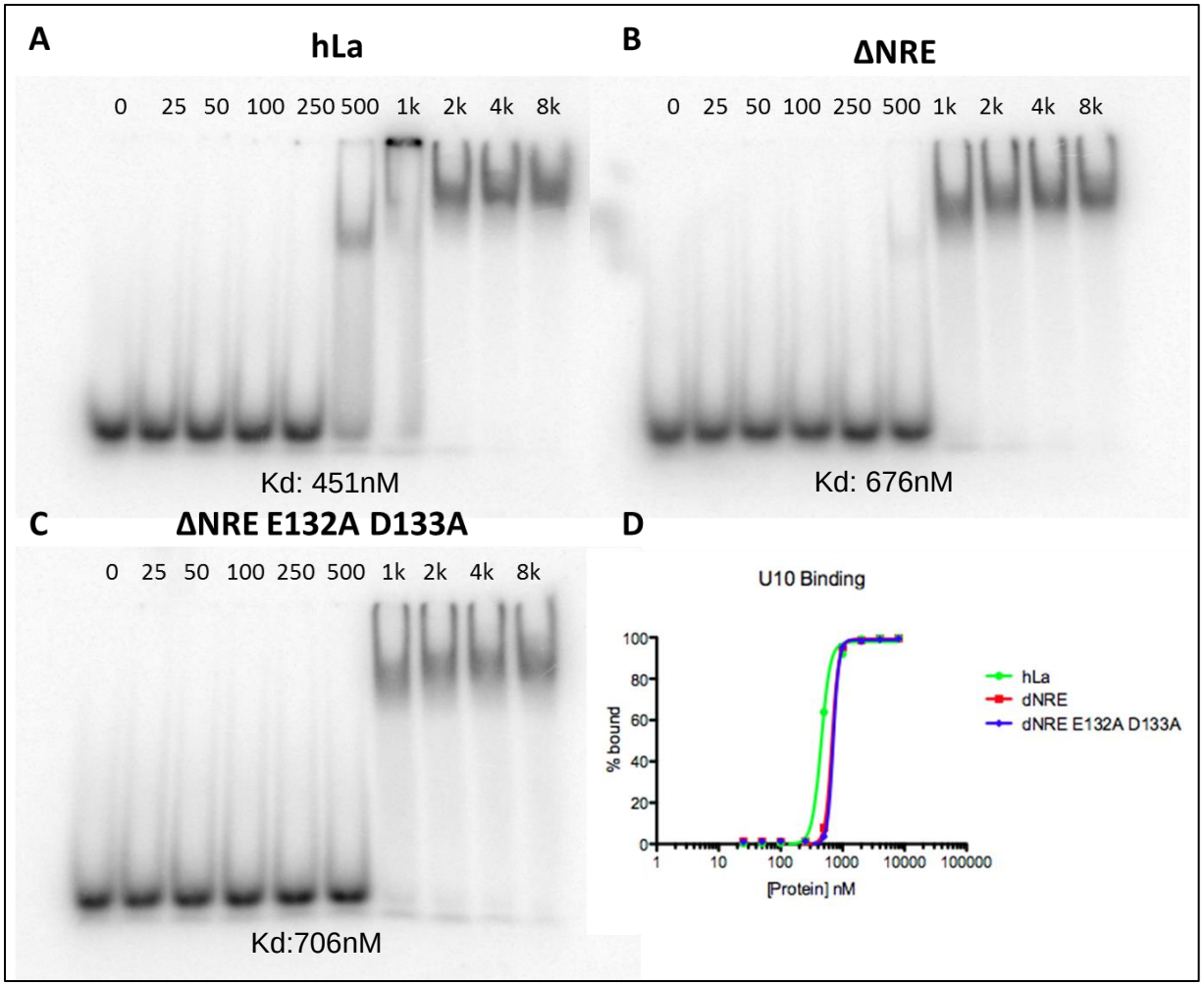

Figure 9: *(A-C) EMSA results displaying wild type hLa, hLa-ΔNRE and the ΔNRE E132A D133A double mutant binding with a radioactively labelled U10 substrate. No substantial changes in substrate binding affinity are witnessed between proteins. (D) Binding curve highlighting the percentage of bound protein over increasing concentrations.*

3.3 hLa's poly A binding mode is unaffected by the removal of its nuclear retention element.

The gel shifts depicted in Figure 10 A-C show hLa, ΔNRE and the double mutant binding to an A20 oligomer to assess La's poly A binding mode. Removal of La's NRE region results in no drop in A20 affinity (Kd: 800nM) when compared to wildtype (Kd: 722nM). Furthermore, the double mutant shows no notable change in A20 affinity (Kd: 954nM) in comparison to wild type. The similarities of Kd values amongst the proteins is evident upon examination the EMSAs. All three proteins show to interact with the A20 oligomer at 1000nM with hLa showing a glimpse of binding at 500nM. In addition, the binding curve in figure 10D illustrates the near identical A20 binding affinity seen with all three proteins. These findings suggest that La's nuclear retention element has no importance in it's poly A binding mode since its removal results in no change in poly A binding affinity.

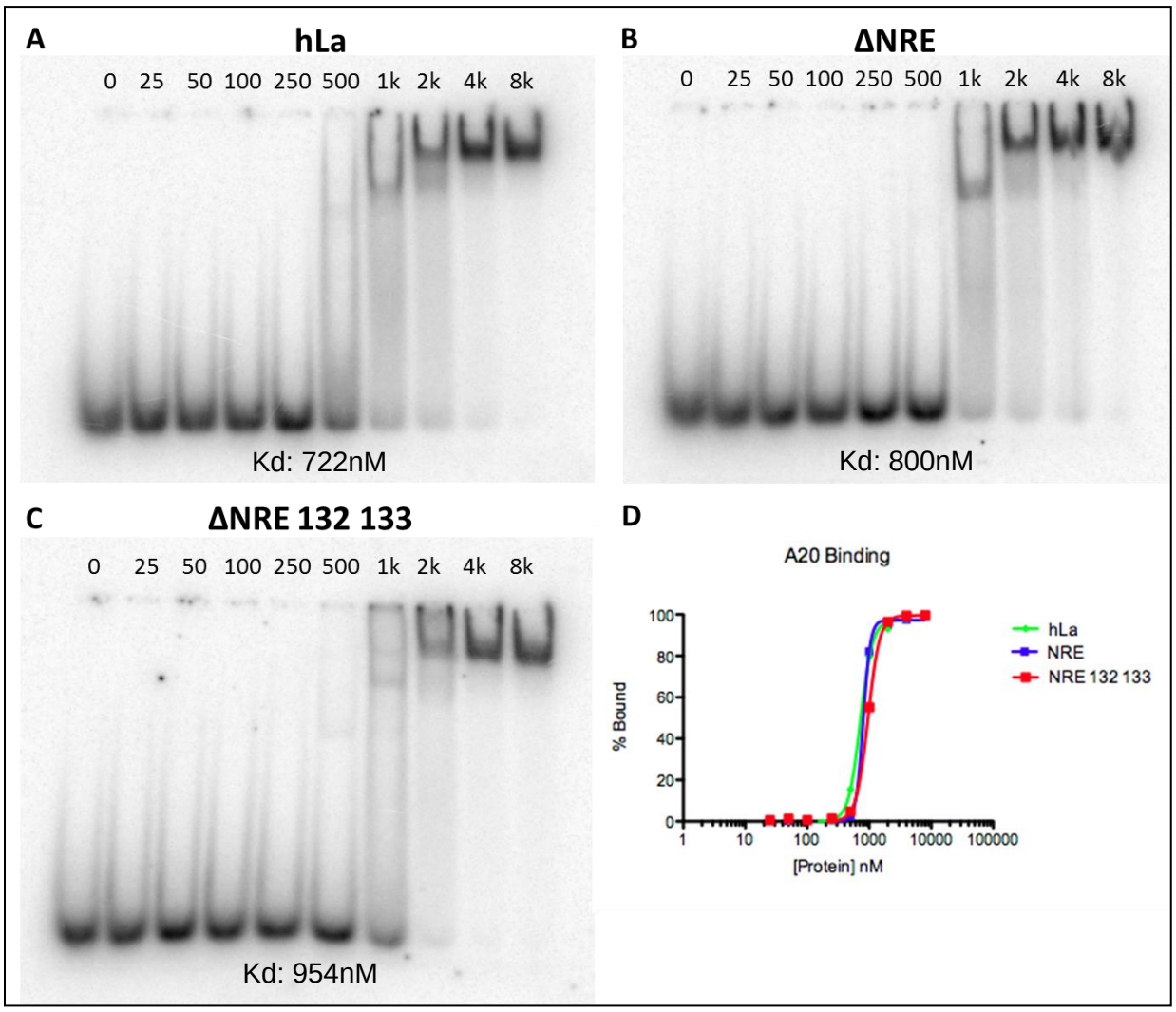

Figure 10: *(A-C) EMSA results displaying wild type hLa, hLa-ΔNRE and the ΔNRE E132A D133A double mutant binding with a radioactively labelled A20 substrate. No change in substrate affinity is observed. All proteins commence binding with the A20 target at 1000nM. (D) Binding curve highlighting the percentage of bound protein over increasing concentrations.*

3.4 ΔNRE and ΔNRE E132A D133A show a reduction in affinity for CGC pre-tRNA binding

hLa's pre-tRNA binding mode was examined in the gel shifts displayed in figures 11 A-C. In comparison to wildtype (Kd: 144nM), the ΔNRE mutant shows nearly a four-fold reduction in pre-tRNA affinity (535nM). At 250nM, wildtype hLa is shown to be completely bound to the pre-tRNA target (11A). This is evident from the lack of free RNA seen in the gel at this concentration. The ΔNRE mutant requires a concentration of 1000nM to achieve this similar leveling of complete binding (11B). The ΔNRE mutant's pre-tRNA affinity reduction is also illustrated by the rightward shift depicted in the binding curve of figure 11D. Surprisingly, the double mutant displays an even further reduction in pre-tRNA affinity (829nM) in comparison to the ΔNRE mutant with complete pre-tRNA binding achieved at 2000nM (11C). It is clear from these data that La's NRE is important for maintaining its ability to efficiently bind to precursor tRNAs. Its removal results in a sharp decline in substrate affinity, which is indicated from the dramatic increases in CGC Kd values for hLa-ΔNRE and double mutants. The lack of any reduction in poly A affinity seen with ΔNRE mutants in Figure 10B in conjunction with the reduction in pre-tRNA affinity observed from these EMSAs lead us to question what happens when ΔNRE mutants are exposed to multiple RNA targets at once? In the presence of multiple RNA targets (an event which would normally occur within the nucleus) do these ΔNRE mutants maintain their engagement with precursor tRNAs or does the reduction in affinity now make them more susceptible to interaction with poly A tails of lesser characterized mRNA targets? This question is examined through competition EMSAs presented in section 3.8.

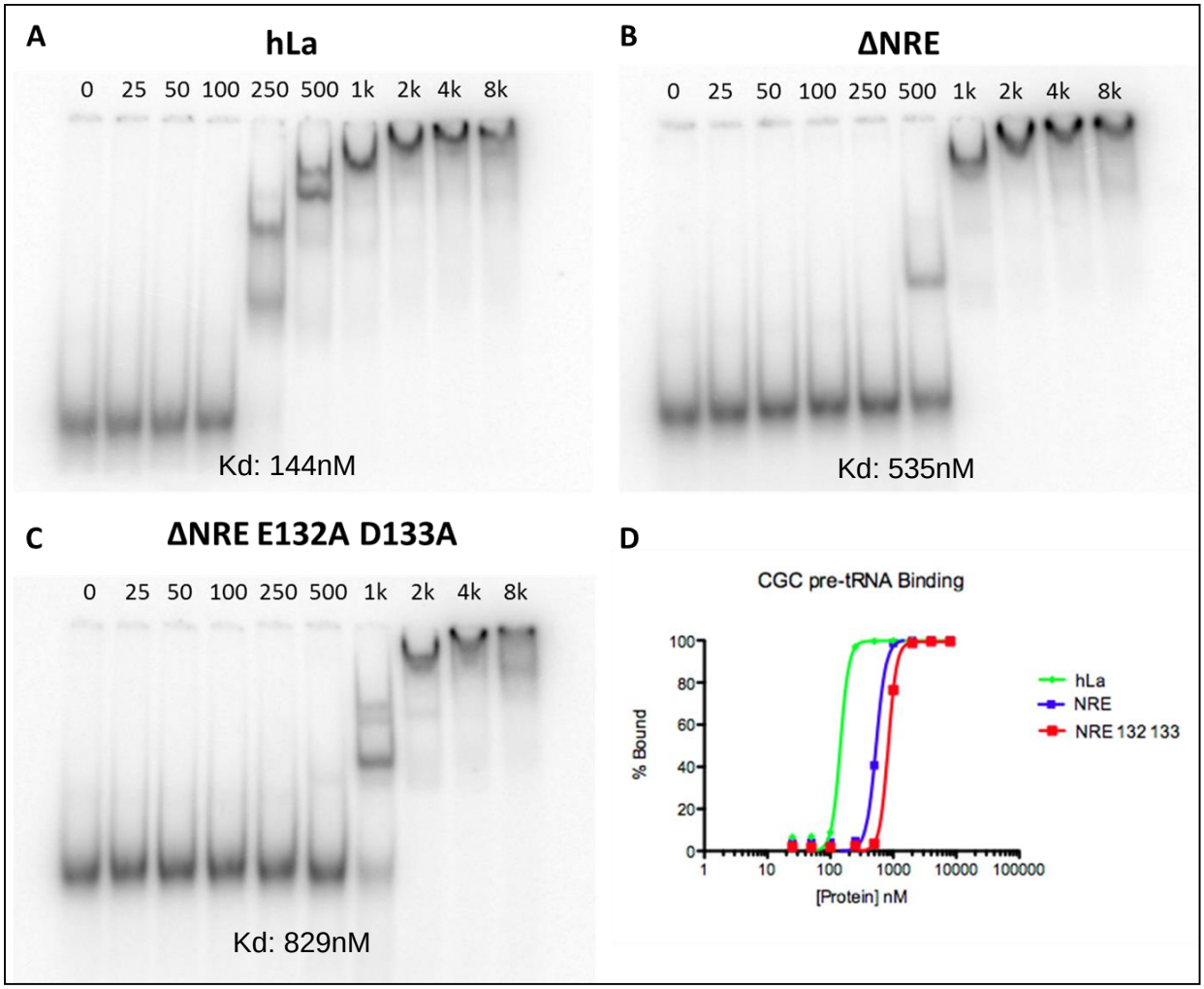

Figure 11: *(A-C) EMSA results displaying wild type hLa, hLa-ΔNRE and the ΔNRE E132A D133A double mutant binding with a radioactively labelled CGC pre-tRNA substrate. A significant reduction in pre-tRNA affinity is witnessed with both hLa-ΔNRE and the ΔNRE double mutant with complete binding of the RNA substrate occurring at 1000nM and 2000nM respectively; compared to wildtype which binds completely at 250nM. (D) Protein binding curves highlighting the percentage of bound protein over increasing concentrations. The rightward shift seen in the ΔNRE (blue) and double mutant (red) binding curves illustrate this reduction in precursor tRNA affinity.*

3.5 Disruption of hLa's salt bridge with the K316E K317E mutant causes no change in its affinity for the U10 oligomer

EMSAs were conducted on the salt bridge disrupting hLa K316E K317E mutant as well as the double swapped hLa E132K D133K K316E K317E mutant to examine the importance this NRE-RRM1 interaction may have on hLa's 3' terminal uridylate binding mode. U10 affinity does not seem falter upon disruption of this salt bridge interaction between the two domains. Both hLa and the K316E K317E mutant display similarities in U10 affinity with Kd values of 451nM and 474nM respectively (Figure 12 A-B). The substantial overlapping of the hLa binding curve (green) and the K316E K317E curve (blue) in figure 12D indicates the near identical binding affinity both proteins share for U10. Moreover, restoration of this inter-domain interaction with the double swapped mutant yields similar affinity to the U10 target (Kd: 539nM) as the aforementioned proteins (12C). These findings suggest that the NRE-RRM1 inter-domain interaction is not required for hLa to recognize and bind to 3' UUU-OH sequences; since the disruption and subsequent restoration of this inter-domain interaction with point mutants shows no difference in U10 affinity (as indicated by the similarities in Kd values).

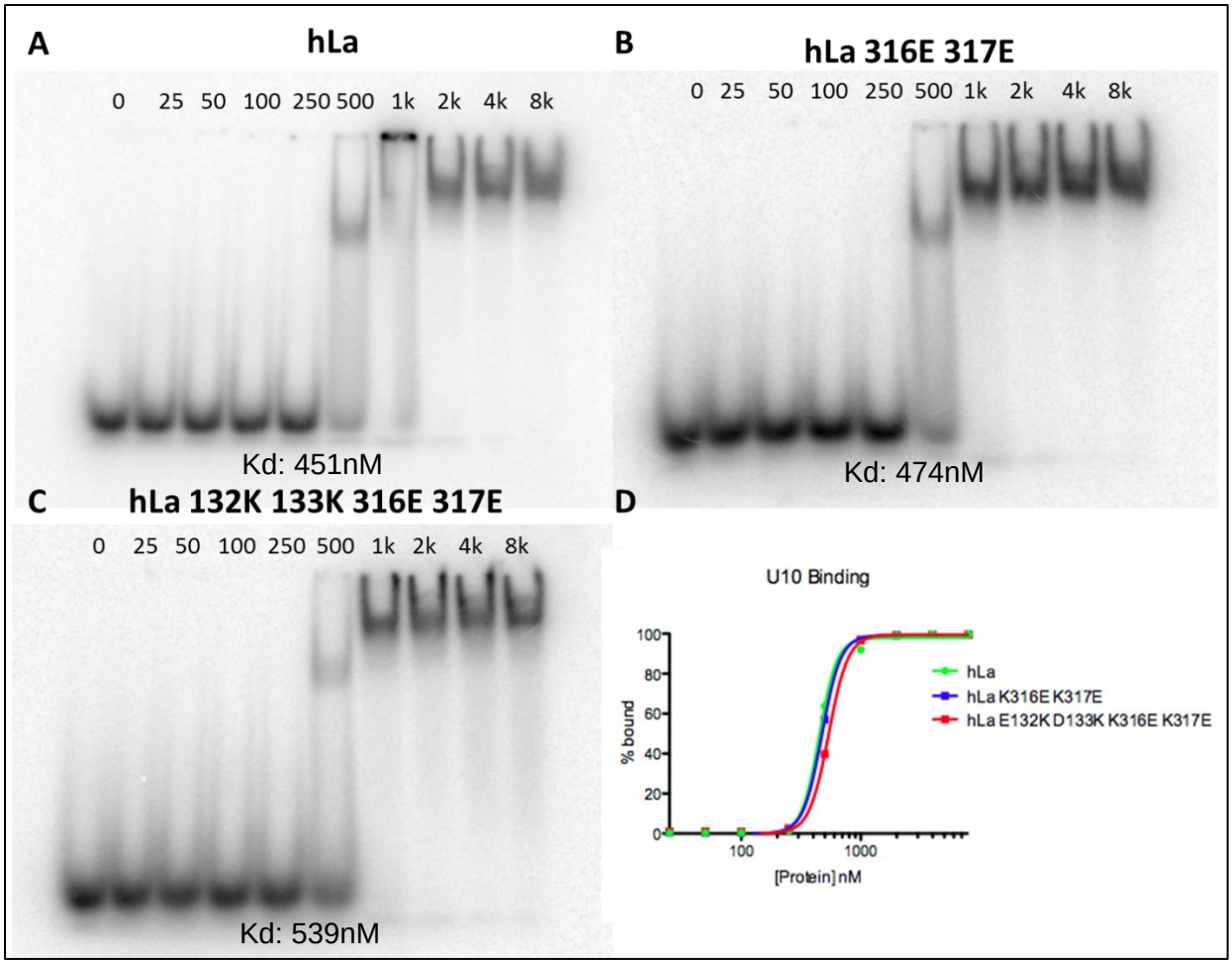

Figure 12: *(A-C) EMSA results displaying wild type hLa, hLa K316E K317E and the double swapped hLa E132K D133K K316E K317E mutant binding with a radioactively labelled U10 substrate. No substantial change in substrate binding affinity was observed amongst proteins. (D) Protein binding curve highlighting the percentage of bound protein over increasing concentrations. The overlapping of binding curves illustrates the similarities in U10 binding between proteins.*

3.6 Disruption of hLa's salt bridge with the K316E K317E mutant causes no change in its affinity for the A20 oligomer

The hLa K316E K317E mutant shows minimal reduction in its affinity for the A20 oligomer (Kd: 869nM) in comparison to wildtype (Kd: 722nM) as shown in figures 13A-B. Moreover, the double swapped mutant (E132K D133K K316E K317E) also shows no change in affinity (Kd: 732nM) as depicted in figure 13C. The similarities of Kd values amongst the proteins is evident upon examination the EMSAs. All three proteins engage with the A20 oligomer at 1000nM and the nearly superimposable binding curves of each protein in figure 13D illustrates this similarity in A20 binding affinity. EMSA data from figure 10 concluded that elimination of hLa's nuclear retention element causes no disruption of its poly A binding mode. Thus, it isn't of much surprise that the ΔNRE-mimicking K316E K317E mutant also shows no disruption of its poly A binding mode. The results from this set of EMSAs confirm the notion that hLa's poly A binding mode remains unaffected upon 1) deletion of its NRE region or 2) the disruption of its salt bridge between NRE and RRM1 domains.

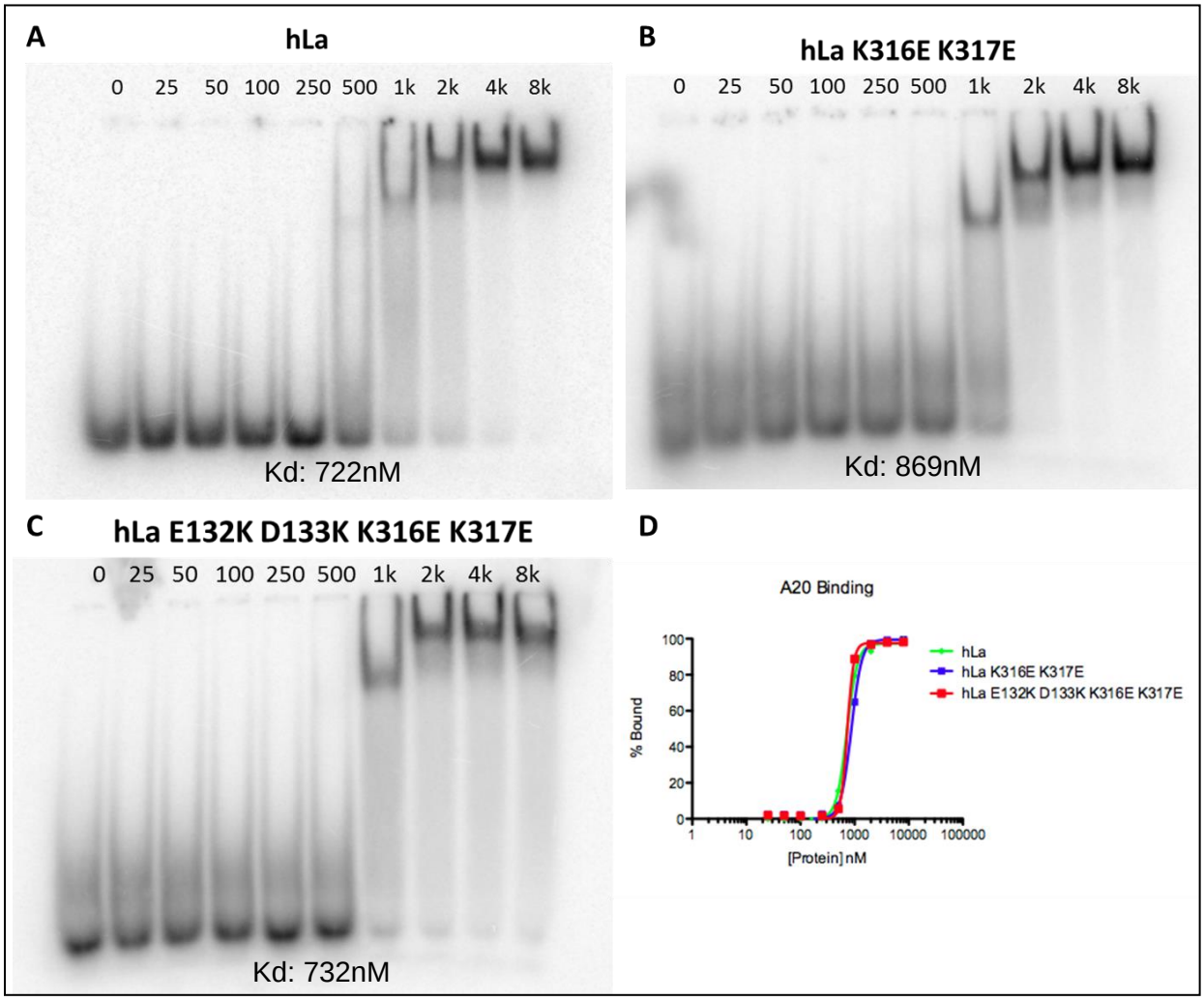

Figure 13: *(A-C) EMSA results displaying wild type hLa, hLa K316E K317E and the double swapped hLa E132K D133K K316E K317E mutant binding with a radioactively labelled A20 substrate. No substantial changes to A20 affinity are witnessed between the examined proteins with target binding beginning at 1000nM. (D)Protein binding curve highlighting the percentage of bound protein over increasing concentrations. The nearly superimposable binding curves highlight the similarities in A20 target affinity.*

3.7 Disruption of hLa's salt bridge with the K316E K317E mutant exhibits a reduction in pre-tRNA affinity that can be partially restored by the E132K D133K K316E K317E mutant

Disruption of hLa's salt bridge interaction with the K316E K317E mutant resulted in a greater than four-fold reduction in pre-tRNA affinity (Kd: 695nM) compared to wildtype (Kd: 144nM). The EMSAs in figure 14 show wild type hLa completely bound to the pre-tRNA substrate at 250nM (14A) whereas the K316E K317E mutant reaches this same level of binding at 1000nM (14B). These findings suggest that the NRE-RRM1 salt bridge may play an important role in pre-tRNA binding since its disruption results in a dramatic reduction in precursor tRNA affinity. In figure 14C, the double substitution mutant hLa E132K D133K K316E K317E shows the ability to restore pre-tRNA binding by almost two-fold (Kd: 412nM). At 500nM, this mutant is almost completely bound to the RNA substrate. The results from this EMSA data set indicate that the K316E K317E mutant may interact with pre-tRNAs in a similar manner as the ΔNRE mutant since both show a similar reduction in pre-tRNA affinity. Furthermore, it would seem from the slight restoration of pre-tRNA binding, the attempts to fix the disrupted salt bridge interaction with the double substitution mutant may have been successful. Full restoration of pre-tRNA binding to the level of wildtype hLa is not seen however, improvement from the K316E K317E mutant is clearly evident.

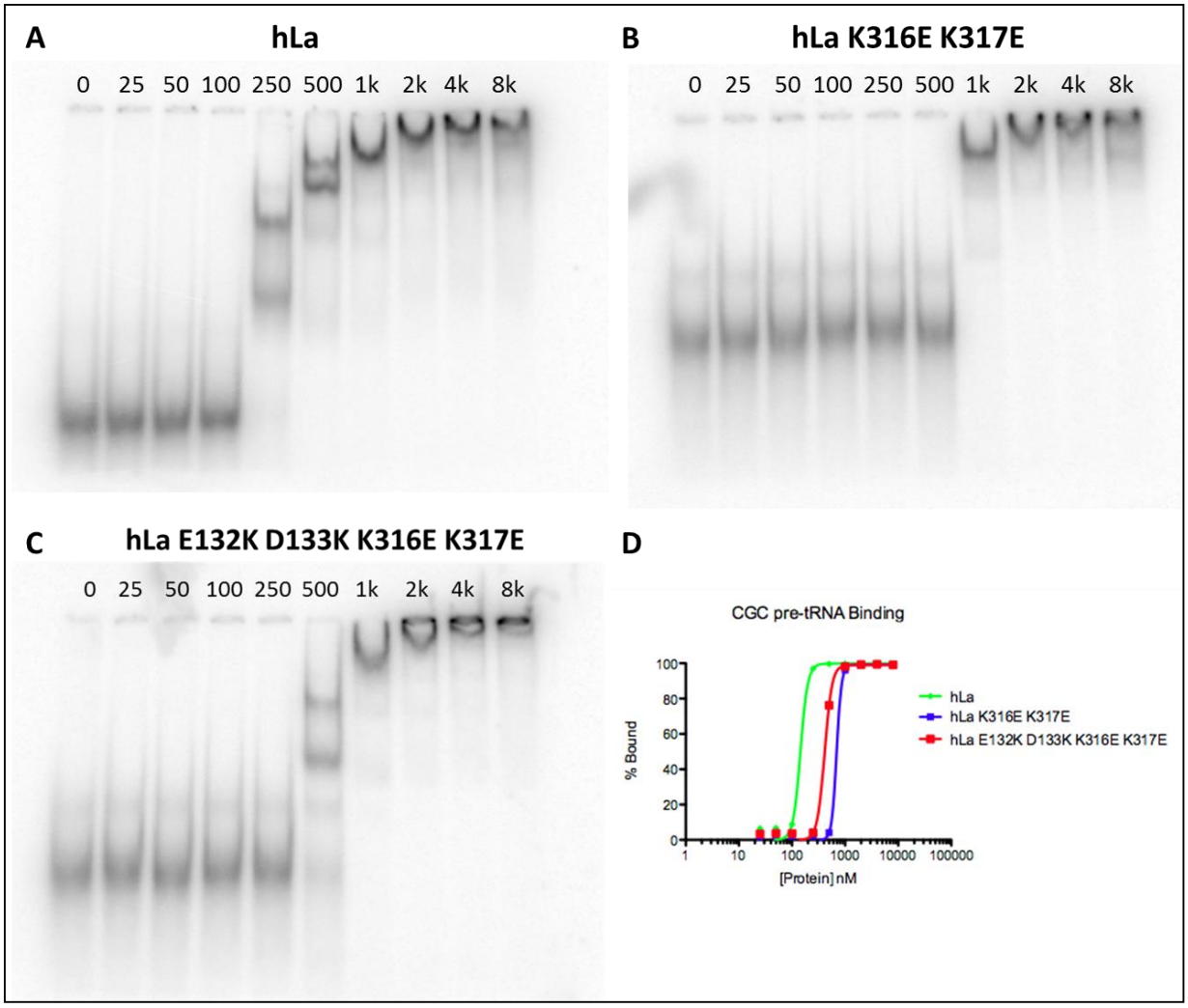

***Figure 14**: (A-C) EMSA results displaying wild type hLa, hLa K316E K317E and the double swapped hLa E132K D133K K316E K317E mutant binding with a radioactively labelled pre-tRNA CGC alanine. Disruption of the hypothesized NRE-RRM1 salt bridge interaction with the K316E K317E mutant causes a 4-fold reduction in precursor tRNA affinity with binding now occurring at 1000nM rather then 250nM seen with wildtype. Attempts to restore this inter-domain interaction by switching the domain locations of the acidic and basic residues resulted in a 2-fold restoration with precursor tRNA binding now occurring at 500nM. (D) Binding curve highlighting the percentage of bound protein over increasing concentrations.*

3.8 Poly U RNA competitor successfully competes off labelled A20 for binding in ΔNRE and hLa K316E K317E mutants

Competition EMSA analysis was conducted to discover how hLa, ΔNRE and the salt bridge mutants behave upon simultaneous exposure to multiple RNA targets. The competition EMSA was set up as followed; Radioactively labelled A20 was used to visualize the interaction with 2uM of protein. Cold U10 and A20 oligomers were added in increasing amounts to examine whether they could compete off the labelled A20 oligo. Cold U10 was added in increasing amounts (0.5-32uM) in Figures 15A-C lanes 4 to 1. The same increasing amounts of cold A20 were added in lanes 7 through 10 and acted as a positive control for RNA binding competition. No protein or competitor were added to lane 5 (NP lane) of the competition EMSA while strictly no competitor was added to lane 6 (NC lane). For all four proteins examined, an increase in the amount of free labelled A20 (seen at the bottom of the gels in lanes 7-10) upon increasing amounts of cold A20 suggests successful competition. The cold A20 oligo competes off the hot A20 oligomer because both bind to the same region on the protein. In figure 15A, the addition of cold U10 in increasing amounts (lanes 4-1) to hLa results in no visible change to A20 binding. From this, it appears that wildtype hLa is locked into a conformation that enables it to bind to poly A's however this conformation does not seem compatible for recognizing 3' UUU-OH sequences. Conversely, when observing the ΔNRE mutant in figure 15B it is evident that A20 begins to get competed off by cold U10 starting at 2uM and increasing as the concentration of U10 increases to 32uM. Such a result would suggest the notion that U10 and A20 are now competing for the same binding site with the elimination of the NRE. The hLa K316E K317E mutant in

figure 15C also displays similar behaviour with addition of cold U10 competing off the radioactively labelled A20. This suggests that the NRE-RRM1 salt bridge may play an important role in controlling hLa's distinct binding modes (either A binding or U binding- not both) and therefore its removal makes the protein more accessible for competition between multiple RNA targets. The double substitution mutant hLa E132K D133K K316E K317E (15D) does not seem to completely restore wildtype behaviour since a small portion of labelled A20 is competed off by increasing amounts of cold U10 however, this competition is not as substantial as that seen with the K316E K317E mutant. The EMSAs in figure 15 A-D were quantified using prism graph pad and the percentage of labelled A20 bound to the proteins was plotted against the increasing concentrations of cold U10 added (Figure 16). The slope of each curve (obtained from the graphing software) indicates the rate of competition between the RNA targets for each protein and are summarized in table 4. Wild type hLa and the double swapped mutant displayed the least amount of competition from the EMSA data and therefore possessed flatter binding curves which corresponds to smaller or "less negative" slopes. In contrary, ΔNRE and hLa K316E K317E showed a larger amount of competition which upon quantification, was illustrated by their steep binding curves and corresponded with larger or "more negative" slopes. These binding curve data provide quantitative values to support the qualitative results seen with the competition EMSAs.

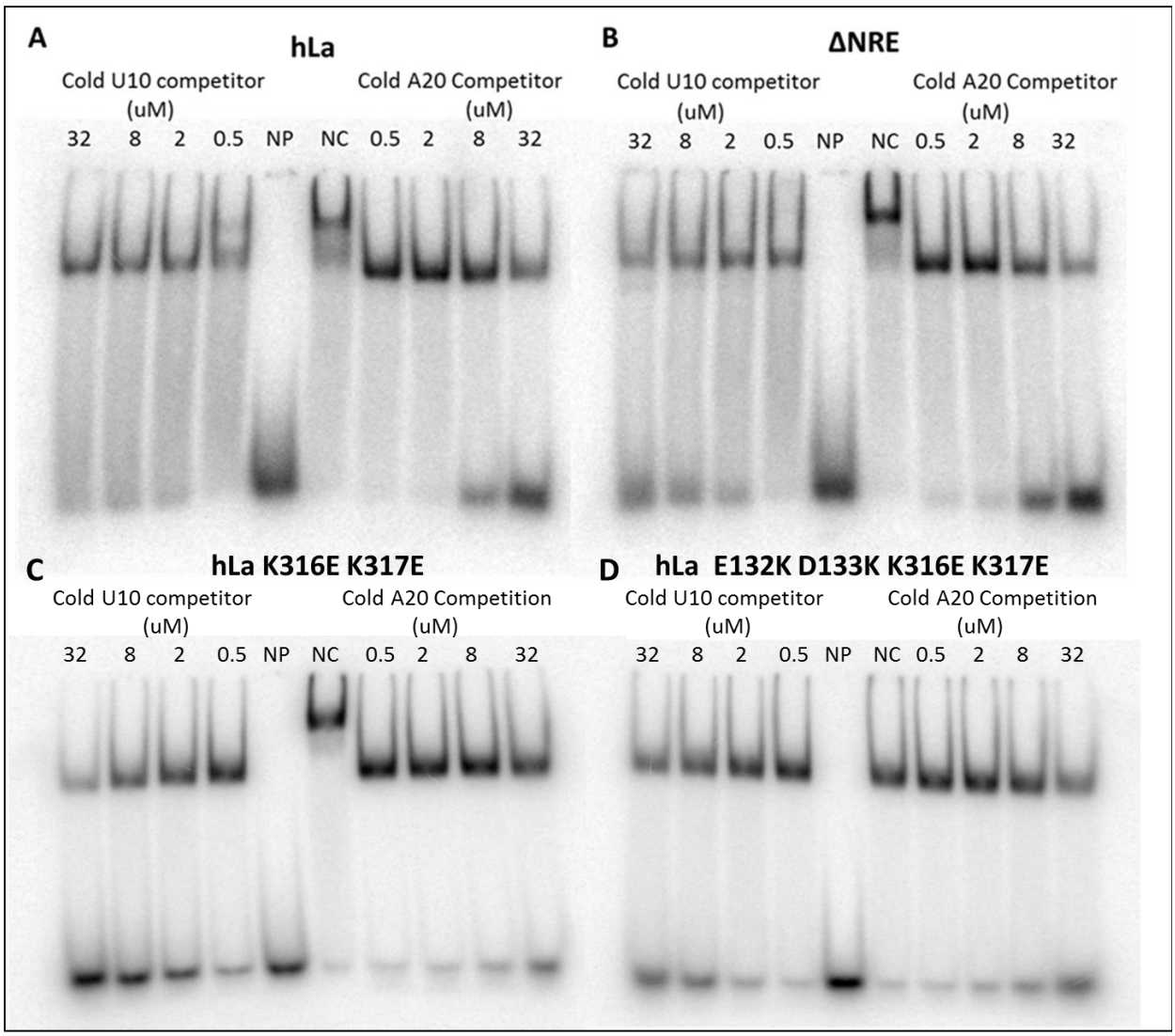

Figure 15: *(A-D) Competition EMSA analysis. 2uM of protein shifting radioactively labeled A20 with increasing amounts of cold U10 (Lanes 4-1) and A20 (Lanes 7-10) competitor. NP refers to no protein or competitor added while NC lanes contain 2uM of protein but no competitor. U10 displays competition of A20 with the ΔNRE and K316E K317E mutants but not with hLa. The double substitution mutant (D) seems to show competition for binding among the two RNAs but to a much lesser extent.*

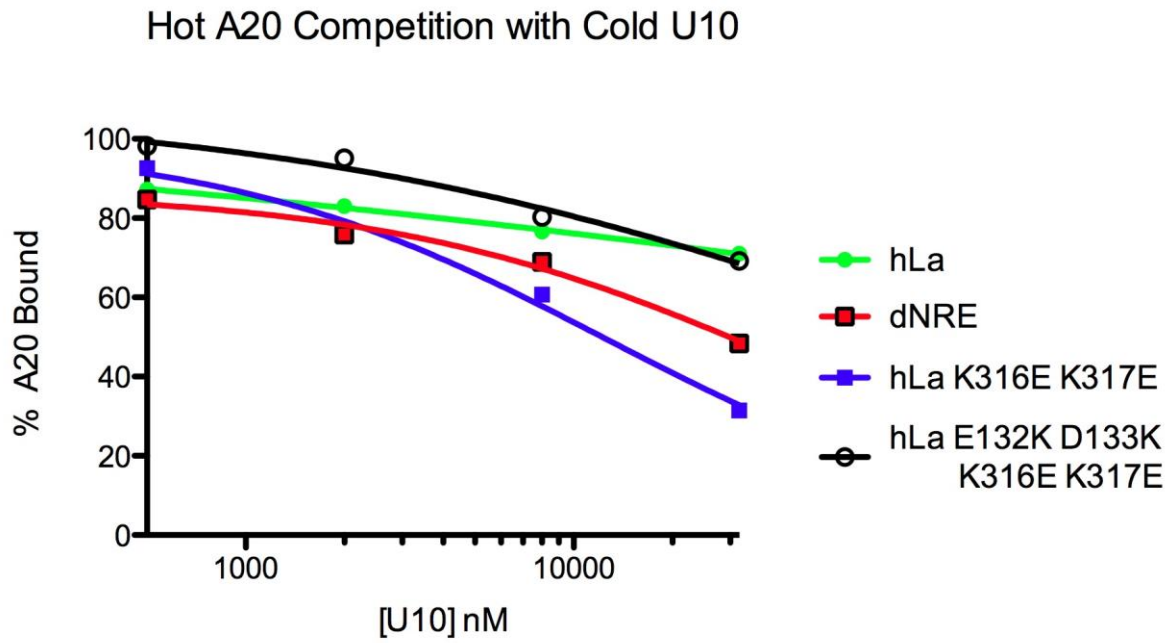

Figure 16: *Percentage of A20 bound to protein plotted against increasing amounts of cold U10 competitor. Data points obtained through quantification of competition EMSAs in figure 15. Prism Graphpad was used to create the binding curves.*

Table 4: *The average slope of each binding curve depicted in figure 16 is summarized in the table below. The average slope, taken from the first and last data point of each curve represents the average rate of competition for binding between U10 and A20 targets. ΔNRE and K316E K317E mutants show the largest negative slope corresponding to the most competition between RNA targets.*

Protein	Slope of binding curve
hLa	**-4.39×10^{-4}**
ΔNRE	**-1.03×10^{-3}**
hLa K316E K317E	**-1.69×10^{-3}**
hLa E132K D133K K316E K317E	**-8.54×10^{-4}**

3.9 CLIP analysis suggests that ΔNRE mutants interact with a greater proportion of poly A substrates than tRNA substrates in vivo.

Cross-linking immunoprecipitation (CLIP) was conducted to identify the abundance of poly A RNA substrates and tRNA substrates interacting with PABP, hLa, ΔNRE and a strictly cytoplasmic variant of hLa known as 1-375 which lacks its nuclear localization signal. Hek293T cells were transfected with either c-myc tagged PABP or GFP tagged hLa, ΔNRE or 1-375. After 24 hours of transfection cells were UV crosslinked and lysed. Appendix H shows the western blot conducted using a sample of each cell lysate. The presence of bands in all tagged protein lanes confirms successful transfection. Magnetic Dynabeads were incubated overnight with 6ug of anti c-myc and GFP antibodies prior to the addition of cell lysate. As a control, a separate set of beads were incubated with 6ug of a control IgG antibody. Half of the cell lysate sample was added to beads containing the appropriate antibody while the other half was added to the beads contain the control IgG. The western blot seen in Appendix I highlights the results of the immunoprecipitation. The size of the c-myc tagged PABP and GFP tagged hLa and mutant variants are approximately 65-70KDa. Bands of this relative size are seen in all + lanes which contain the appropriate c-myc or GFP antibody. This western confirms the successful pulldown of tagged proteins. Pulldown samples were then treated with proteinase K to eliminate all protein leaving only the interacting nucleic acids remaining. These samples were transferred onto a nitrocellulose membrane for northern blot analysis. Figure 17A shows the northern blot results using a dt40 probe which binds to all poly A containing RNA substrates. PABP served as a positive control for strictly poly A substrate binding while 1-375 was used to identify the abundance of

poly A substrates pulled down by a strictly cytoplasmic mutant. These two proteins show the greatest amount of poly A substrate pulldown (Figure 17 lanes 3 and 9) with PABP pulling down the largest amount of poly A substrates. Both hLa and ΔNRE mutants pull down poly A however nonspecific poly A pulldown is also seen in the control IgG antibody lanes (- lanes) of these proteins. Figure 17B shows the northern blot results using a Met tRNA probe. As expected, no tRNA substrates are pulled down with PABP. Moreover, a relatively equal amount of tRNAs are pulled down with hLa and ΔNRE which represent the most of the examined proteins while very little tRNAs are pulled down with the cytoplasmic mutant. Prior to quantification, the band intensities seen in all (+) lanes were subtracted by the intensity values obtained from their respective control (-) lane in order to normalize the data and eliminate the effect on non-specific binding. After quantification, dt40 band intensity for each protein were divided by their respective Met tRNA intensity to obtain a ratio. These ratios represent the proportion of poly A substrates to tRNA substrates pulled down by each protein and were plotted on the bar graph in figure 18. PABP shows the highest dt40/Met tRNA ratio suggesting that these proteins pulled down a substantially greater amount of poly A RNAs to tRNAs. The second largest ratio is obtained by the 1-375 mutant. Considering this mutant is only present in the cytoplasm it exposure to poly A tails from mRNAs would far exceed exposure to Met tRNAs. Finally, ΔNRE mutants seems to have a larger dt40/Met tRNA ratio in comparison to wild type hLa. This may suggest that in vivo, ΔNRE mutants are interacting with poly A containing RNAs to a greater extent than tRNAs, specifically Met tRNAs.

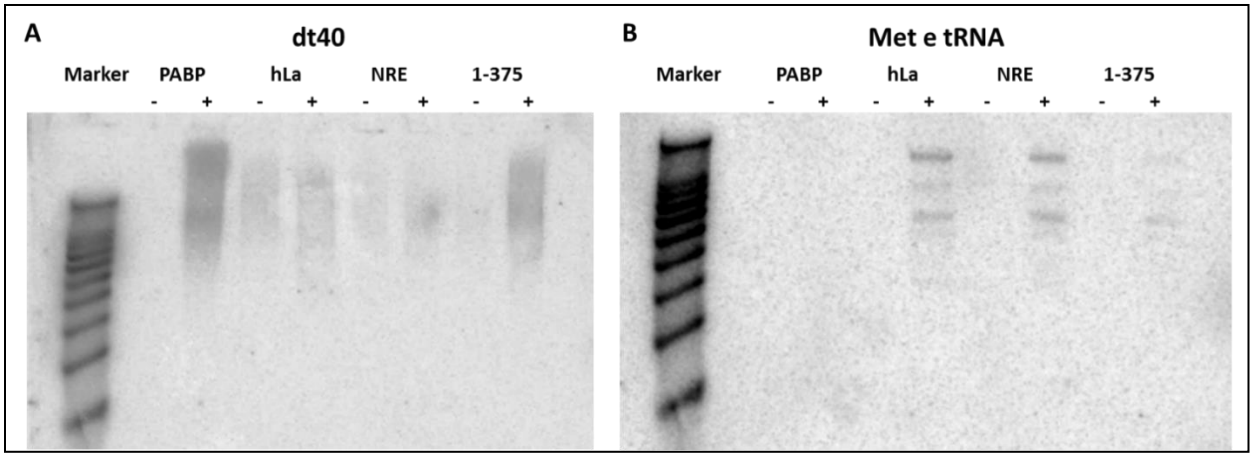

Figure 17: *Crosslinking immunoprecipitation northern blot probing for poly A sequences using dt40 (A) and human methionine tRNA (B). Hek293T cells transfected with either c-Myc tagged PABP or GFP-tagged hLa, ΔNRE or hLa 1-375 were UV crosslinked and immunoprecipitated with either control IgG antibody (- lanes) or their respective c-myc and GFP antibodies (+ lanes).*

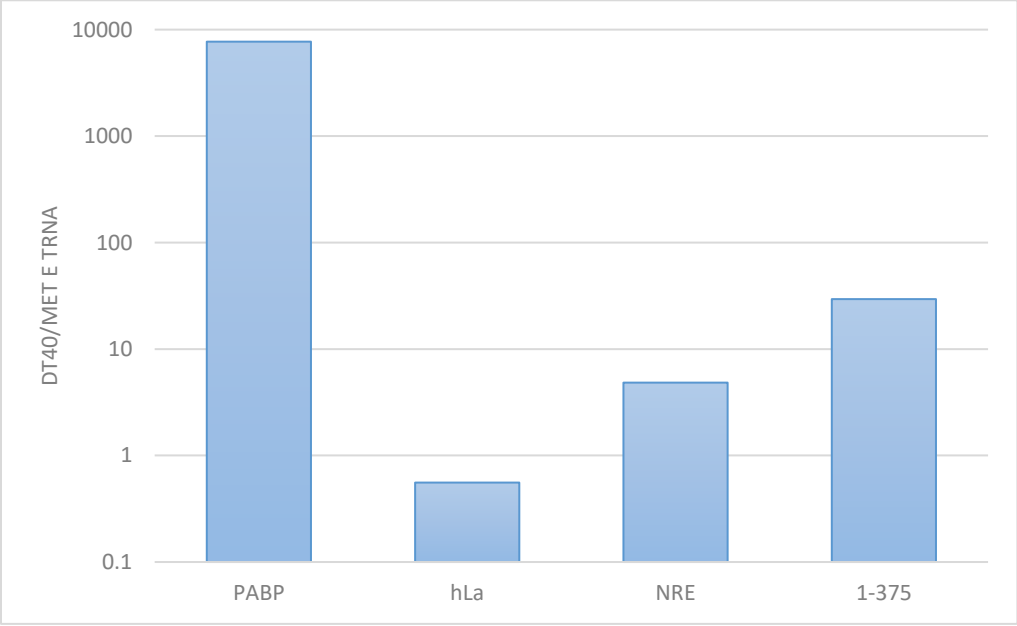

Figure 18: *Quantification of northern blot results seen in figure 17. All values were normalized by subtracting the intensities of the control (-) lanes from the (+) lanes. Normalized Met tRNA intensities were divided from dt40 values to obtain a ratio of poly A sequences to methionine tRNA sequences pulled down for each protein.*

DISCUSSION

4.1 hLa's 3' UUU-OH binding mode remains unaffected upon NRE deletion

The initial findings from the U20 EMSA data set suggesting a reduction in 3' UUU-OH binding with hLa-ΔNRE raised suspicion as to whether this was truly a reduction in the U binding mode or if this was due to the fact that being sufficiently long enough, the U20 was making additional contacts on hLa that were not possible on the NRE lacking mutant. Examination of U10 binding addressed this problem and showed that no differences in affinity where now witnessed between hLa-ΔNRE and wildtype. Similar findings regarding U10 binding were also seen with hLa K316E K317E and the double substituted hLa E132K D133K K316E K317E when compared to wildtype. These data enable us to conclude that removal of the NRE nor the disruption of the NRE-RRM1 salt bridge affects La's 3' UUU-OH recognition. Although these findings may appear as null results, they do help improve our understanding of how hLa engages with it's 3' UUU-OH containing RNA targets. Until now, published data has only showed hLa's conserved NTD interacting with these targets [6]; the solved crystal structure highlighting this interaction did not contain the protein's CTD where the NRE is located. Our U10 EMSA data allows us to can expand on this current understanding by confirming that hLa's NRE has no role in binding with 3' terminal uridylate sequences.

The limitation presented with using a poly U oligo for binding is that such sequences alone do not exist in nature. However, these sequences are found on the

ends of all pol III transcripts which hLa is known to bind to therefore, the use of a U10 oligomer allowed us to examine this interaction in a simplified manner.

4.2 Removal or mutation of hLa's NRE homogenizes the poly A binding mode with its 3'UUU-OH binding

Binding affinity for the A20 oligomer showed no change upon disruption of hLa's NRE-RRM1 salt bridge or elimination of it's NRE entirely. Compared to hLa's 3'UUU-OH binding and precursor tRNA binding, the poly A binding mode is less characterized. Despite this, it is currently understood that the LAM, RRM1 and RRM2 all play a role in A20 binding since elimination or mutation to these domains results in a reduction in A20 affinity (unpublished lab data). Therefore, it does not come as a complete surprise that elimination of the NRE or the mutations made to it (K316E K317E) resulted in no change in poly A affinity.

In spite of this, hydrogen deuterium mass spectrometry analysis (H/D exchange) from a collaborating lab tells a different story. Using H/D exchange, our collaborators examined how the structural domains of hLa and hLa-ΔNRE change when bound to a U10 and A20 RNA substrate. They discovered that removal of the NRE helix causes these mutants to bind to A20 targets as if they were U10. This contrasted wildtype which displayed two separate H/D exchange patterns when bound to U10 and A20 suggesting separate binding modes. These findings strongly suggest that elimination of the NRE results in a homogenization of hLa's 3'UUU-OH binding mode and its poly A binding mode. Further H/D exchange analysis on hLa K316E K316E produced similar findings indicating a homogenization between said binding modes. Conversely,

examination of hLa E132K D133K K316E K317E generated two separate H/D exchange patterns similar to those seen with wildtype suggesting that restoration of the NRE-RRM1 salt bridge in turn restores this separation of binding modes. Interestingly, the findings from our collaborators can be used to explain the results observed from our competition EMSAs. Homogenization of the 3'UUU-OH binding mode with it's poly A binding would make hLa-ΔNRE and hLa K316E K317A mutants more susceptible to competition when presented with U10 and A20 since these proteins would bind both targets the same way. The competition EMSA data supports this, with both hLa-ΔNRE and hLa K316E K317A mutants showing the greatest amount of competition between targets while wildtype and hLa E132K D133K K316E K317E show minimal to no competition.

These data do however highlight a limitation with the usage of EMSAs to assess protein interaction. Although EMSAs provide us with differences in affinity for binding targets, they do not give detailed information as to how the protein is interacting with its target. Our EMSA data revealed no differences in A20 affinity between hLa and ΔNRE however the H/D exchange data from our collaborators shows that although affinity does not change, the way hLa-ΔNRE engages with these targets has.

4.3 hLa's NRE contains an indirect yet important role in precursor tRNA binding

The substantial differences in RNA target binding between hLa and hLa-ΔNRE mutants were seen when examining the precursor tRNA binding mode. Deletion of the NRE resulted in a substantial drop in pre-tRNA affinity. Moreover, mutations made to

the NRE (K316E K317E) also resulted in a dramatic decrease in pre-tRNA affinity compared to wildtype. Our U10 EMSA data indicates that no changes to 3'UUU-OH binding exists between hLa and the mutants tested thus, it can be concluded that these differences in pre-tRNA binding are not due to deficiencies in binding the 3' trailer of the pre-tRNA. These data suggest that hLa's NRE either makes direct contact with the body of the pre-tRNA to stabilize the interaction or indirectly ensures the protein maintains a favourable conformation to bind pre-tRNAs. To date, only two other domains of hLa are known to make direct contact with the pre-tRNA aside from the La module binding the 3' trailer sequence. The loop 3 region of the RRM1 comprised of amino acids 143-151 directly interact with the body of the pre-tRNA while the SBM located directly after the NRE binds to the 5' leader of the pre-tRNA with high affinity unless phosphorylated at serine 366. If NRE were to play a direct role in binding, its elimination or mutation should result in an irreversible loss of affinity for pre-tRNA substrates. However, this is not the case since pre-tRNA binding can be restored 2-fold in hLa K316E K317E mutants by changing the acidic residues in the RRM1 to basic lysine residues (hLa E132K D133K K316E K317E). These findings suggest an indirect role played by the NRE; one that relies on contacts made between acidic residues of the RRM1 (132 and 133) and basic lysine residues at positions 316 and 317 to promote a structural conformation that is favourable for pre-tRNA binding. The disruption of this inter-domain interaction either through point mutation to the NRE or its removal entirely causes a reduction in pre-tRNA binding affinity because the protein can no longer maintain a conformation that supports interaction with the body of the pre-tRNA. By switching the location of these charged residues but maintaining the potential for inter-domain

interaction, pre-tRNA binding affinity is partially restored. This emphasizes the indirect yet crucial role NRE possess; maintaining proper pre-tRNA binding through contains with the RRM1 so that subsequent processing can occur.

4.4 Proposing a model for the inappropriate nuclear export of hLa-ΔNRE

The CLIP assay provided us with an in vivo approach to examine the type of RNAs interacting with hLa and hLa-ΔNRE. Results from this experiment indicated that hLa-ΔNRE mutants were immunoprecipitated with a greater proportion of poly A messages bound to them than tRNAs. Our pre-tRNA and A20 EMSA data can be used to provide an explanation for these results. A20 EMSA data revealed no changes in binding affinity between hLa and hLa-ΔNRE however it was discovered through H/D exchange data of our collaborators that hLa-ΔNRE mutants bind to poly A and poly U sequences identically. In addition to this newly generated competition for binding between poly A and U targets hLa-ΔNRE mutants also display a substantial reduction in pre-tRNA binding affinity in comparison with wildtype. Taken together, these data suggest that in the nucleus where proteins are exposed to an abundance of RNAs, hLa-ΔNRE mutants may now be more susceptible to binding poly A messages since 1) these messages now compete for the same site as the 3’ trailer of pre-tRNAs and 2) pre-tRNA binding is notably reduced. The consequence for binding to the poly A tail of an mRNA target instead of a pre-tRNA is that these mutants are now inappropriately exported from the nucleus. The mechanism for export is crm1 dependant since inhibition via LMB restores the proteins nuclear phenotype. Thus it is hypothesized that

mRNAs exported in a crm1 dependant manner would be clear targets for hLa-ΔNRE binding.

This model does contain some limitations; one of which is that it can not be used to explain the nuclear restoration seen with ΔNRE E132A D133A double mutant in previous literature. A20 EMSA data shows no difference in affinity however H/D exchange analysis was not conducted on this mutant thus no additional information as to how this mutant may specifically interact with an A20 target is available. In addition, this mutant's pre-tRNA binding displayed a greater drop in affinity compared to hLa-ΔNRE. Therefore, using the rationale from the proposed model, this mutant should be cytoplasmic but in reality it is nuclear. Despite this, the proposed model attempts to provide a simplistic explanation for the cytoplasmic phenotype seen with hLa-ΔNRE that not only is supported by the EMSAs conducted but also by the CLIP data.

FUTURE PERSPECTIVES

Due to the similarities in RNA binding behaviours of hLa-ΔNRE and hLa K316E K317E, it would be of interest to conduct a CLIP on cells overexpressing hLa K316E K317E as well as the double substitution mutant hLa E132K D133K K316E K317E. Due to their similarities in RNA target binding it would be hypothesized that cells expressing hLa K316E K317E immunoprecipitate with greater proportion of mRNAs bound to them than tRNAs, similar to what was observed with hLa-ΔNRE. In contrast, due to the restoration in RNA target affinity, it is hypothesized that hLa E132K D133K K316E K317E mutants would be able to restore RNA target preference back to what was witnessed with wildtype hLa. These experiments could be used to confirm the importance that the NRE-RRM1 inter-domain interaction has on maintaining pre-tRNA binding affinity in vivo as all current data used to propose this has been completed in-vitro through EMSAs as well as H/D exchange analysis from our collaborators.

To address whether protein-protein interactions have a designated role in mediating hLa's intracellular phenotype, Hek 293T cells overexpressing hLa and hLa-ΔNRE were immunoprecipitated and these complexes sent for HPLC mass spectrometry analysis to identify any differences in the protein pulled down. Furthermore, additional samples were sent after RNAse treatment to eliminate any protein bound to hLa or hLa-ΔNRE that may be mediated through an RNA sequence. Unfortunately, we are still waiting on the results from said experiments from our collaborator therefore, no additional comments can be made at this point.

REFERENCES

1. Bousquet-Antonelli, C., & Deragon, J.-M. (2009). A comprehensive analysis of the La-motif protein superfamily. *RNA*, *15*(5), 750–764.

2. Mattioli, M. and Reichlin, M. (1974), Heterogeneity of RNA protein antigens reactive with sera of patients with systemic lupus erythematosus description of a cytoplasmic nonribosomal antigen. Arthritis & Rheumatism, 17: 421–429.

3. Park, J.-M., Kohn, M. J., Bruinsma, M. W., Vech, C., Intine, R. V., Fuhrmann, S., … Maraia, R. J. (2006). The Multifunctional RNA-Binding Protein La Is Required for Mouse Development and for the Establishment of Embryonic Stem Cells. *Molecular and Cellular Biology*, *26*(4), 1445–1451.

4. Yoo, C. J., & Wolin, S. L. (1994). La proteins from Drosophila melanogaster and Saccharomyces cerevisiae: a yeast homolog of the La autoantigen is dispensable for growth. *Molecular and Cellular Biology*, *14*(8), 5412–5424.

5. Van Horn, D. J., Yoo, C. J., Xue, D., Shi, H., & Wolin, S. L. (1997). The La protein in Schizosaccharomyces pombe: a conserved yet dispensable phosphoprotein that functions in tRNA maturation. *RNA*, *3*(12), 1434–1443.

6. Teplova, M., Yuan, Y.-R., Phan, A. T., Malinina, L., Ilin, S., Teplov, A., & Patel, D. J. (2006). Structural Basis for Recognition and Sequestration of UUU_{OH} 3′ Temini of Nascent RNA Polymerase III Transcripts by La, a Rheumatic Disease Autoantigen. *Molecular Cell*, *21*(1), 75–85.

7. Stefano, J.E. (1984) Purified lupus antigen la recognizes an oligouridylate stretch common to the 3′ termini of RNA polymerase III transcripts. *Cell,* 36(1) 145-154.

8. Bayfield, M. A., Kaiser, T. E., Intine, R. V., & Maraia, R. J. (2007). Conservation of a Masked Nuclear Export Activity of La Proteins and Its Effects on tRNA Maturation . *Molecular and Cellular Biology*, *27*(9), 3303–3312.

9. Cléry, A., Blatter, M., Allain, F. H-T. (2008) RNA recognition motifs: boring? Not quite, *Current Opinion in Structural Biology*, 18(3) 290-298.

10. Maris, C., Dominguez, C. and Allain, F. H.-T. (2005), The RNA recognition motif, a plastic RNA-binding platform to regulate post-transcriptional gene expression. FEBS Journal, 272: 2118–2131.

11. Dong, G., Chakshusmathi, G., Wolin, S. L., & Reinisch, K. M. (2004). Structure of the La motif: a winged helix domain mediates RNA binding via a conserved aromatic patch. *The EMBO Journal*, *23*(5), 1000–1007.

12. Wah, D.A., Hirsch, J.A., Dorner, L.F., Schildkraut, I., Aggarwal, A.K. (1997) Structure of the multimodular endonuclease FokI bound to DNA. *Nature* 388(1) 97-100.

13. Rinke, J., Steitz, J.A. (1982) Precursor molecules of both human 5S ribosomal RNA and transfer RNAs are bound by a cellular protein reactive with anti-La Lupus antibodies. *Cell*, 29(1) 149-159.

14. Boire, G., & Craft, J. (1990). Human Ro ribonucleoprotein particles: characterization of native structure and stable association with the La polypeptide. *Journal of Clinical Investigation*, *85*(4), 1182–1190.

15. He, N., Jahchan, N.S., Hong, E., Li, Q., Bayfield, M.A., Maraia, R.J., Luo, K., Zhou, Q. (2008). A La-Related Protein Modulates 7SK snRNP Integrity to Suppress P-TEFb-Dependent Transcriptional Elongation and Tumorigenesis. *Molecular Cell,* 29(5) 588-599.

16. Yoo, C.J., Wolin, S.L. (1997). The Yeast La Protein Is Required for the 3′ Endonucleolytic Cleavage That Matures tRNA Precursors, *Cell,* 89(3) 393-402.

17. Mathews, M. B., & Francoeur, A. M. (1984). La antigen recognizes and binds to the 3'-oligouridylate tail of a small RNA. *Molecular and Cellular Biology*, *4*(6), 1134–1140.

18. Reddy, R., Henning, D., Tan, E., Busch, H. (1983). Identification of a La protein binding site in a RNA polymerase III transcript (4.5 I RNA), *Journal of Biological Chemistry*, 258 8352–8356.

19. Huang, Y., Intine, R. V., Mozlin, A., Hasson, S., & Maraia, R. J. (2005). Mutations in the RNA Polymerase III Subunit Rpc11p That Decrease RNA 3′ Cleavage Activity Increase 3′-Terminal Oligo(U) Length and La-Dependent tRNA Processing. *Molecular and Cellular Biology*, *25*(2), 621–636.

20. Huang, Y., Bayfield, M.A., Intine, R.V., Maraia, R.J. (2006). Separate RNA-binding surfaces on the multifunctional La protein mediate distinguishable

activities in tRNA maturation, *Nature Structural and Molecular Biology*, 13 611–618.

21. Copela, L. A., Fernandez, C. F., Sherrer, R. L., & Wolin, S. L. (2008). Competition between the Rex1 exonuclease and the La protein affects both Trf4p-mediated RNA quality control and pre-tRNA maturation. *RNA*, *14*(6), 1214–1227.

22. Bayfield, M. A., & Maraia, R. J. (2009). Precursor-product discrimination by La protein during tRNA metabolism. *Nature Structural & Molecular Biology*, *16*(4), 430–437.

23. Chakshusmathi, G., Kim, S. D., Rubinson, D. A., & Wolin, S. L. (2003). A La protein requirement for efficient pre-tRNA folding. *The EMBO Journal*, *22*(24), 6562–6572.

24. Anderson, J., Phan, L., Cuesta, R., Carlson, B. A., Pak, M., Asano, K., … Hinnebusch, A. G. (1998). The essential Gcd10p–Gcd14p nuclear complex is required for 1-methyladenosine modification and maturation of initiator methionyl-tRNA. *Genes & Development*, *12*(23), 3650–3662.

25. Bayfield, M. A., Yang, R., & Maraia, R. J. (2010). Conserved and divergent features of the structure and function of La and La-related proteins (LARPs). *Biochimica et Biophysica Acta*, *1799*(5-6), 365–378.

26. Jacks, A., Babon, J., Kelly, G., Manolaridis, I., Cary, P.D., Curry, S., Conte, M. R. (2003). Structure of the C-Terminal Domain of Human La Protein Reveals a Novel RNA Recognition Motif Coupled to a Helical Nuclear Retention Element. *Structure*, 11(7) 833-843.

27. Fok, V., Friend, K., & Steitz, J. A. (2006). Epstein-Barr virus noncoding RNAs are confined to the nucleus, whereas their partner, the human La protein, undergoes nucleocytoplasmic shuttling. *The Journal of Cell Biology*, *173*(3), 319–325.

28. Intine, R.V.A., Sakulich, A.L., Koduru, S.B., Huang, Y., Pierstorff, E., Goodier, J.L., Phan, L., Maraia, R.J. (2000). Control of Transfer RNA Maturation by Phosphorylation of the Human La Antigen on Serine 366, *Molecular Cell*, 6(2) 339-348.

29. Horke, S., Reumann, K., Schweizer, M., Will, H., Heise, T. (2004). Nuclear Trafficking of La Protein Depends on a Newly Identified Nucleolar Localization Signal and the Ability to Bind RNA. *The Journal of Biological Chemistry*, 279(25) 26563-26570.

30. Intine, R.V., Dundr, M., Misteli, T., Maraia, R.J. (2002). Aberrant nuclear trafficking of La protein leads to disordered processing of associated precursor tRNAs, *Molecular Cell*, 9(5) 1113–1123.

31. Xue, D., Rubinson, D. A., Pannone, B. K., Yoo, C. J., & Wolin, S. L. (2000). U snRNP assembly in yeast involves the La protein. *The EMBO Journal*, *19*(7), 1650–1660.

32. Craig, A. W., Svitkin, Y. V., Lee, H. S., Belsham, G. J., & Sonenberg, N. (1997). The La autoantigen contains a dimerization domain that is essential for enhancing translation. *Molecular and Cellular Biology*, *17*(1), 163–169.

33. Stavraka, C., & Blagden, S. (2015). The La-Related Proteins, a Family with Connections to Cancer. *Biomolecules*, *5*(4), 2701–2722.

34. Burrows, C., Abd Latip, N., Lam, S.-J., Carpenter, L., Sawicka, K., Tzolovsky, G., … Blagden, S. P. (2010). The RNA binding protein Larp1 regulates cell division, apoptosis and cell migration. *Nucleic Acids Research*, *38*(16), 5542–5553.

35. Blagden, S.P., Gatt, M.K., Archambault, V., Lada, K., Ichihara, K., Lilley, K.S., Inoue, Y.H., Glover, D.M. (2009). Larp associates with poly(A)-binding protein and is required for male fertility and syncytial embryo development. *Developmental Biology*, 334(1) 186-197.

36. Yang, R., Gaidamakov, S. A., Xie, J., Lee, J., Martino, L., Kozlov, G., … Maraia, R. J. (2011). La-Related Protein 4 Binds Poly(A), Interacts with the Poly(A)-Binding Protein MLLE Domain via a Variant PAM2w Motif, and Can Promote mRNA Stability . *Molecular and Cellular Biology*, *31*(3), 542–556.

37. Schäffler, K., Schulz, K., Hirmer, A., Wiesner, J., Grimm, M., Sickmann, A., & Fischer, U. (2010). A stimulatory role for the La-related protein 4B in translation. *RNA*, *16*(8), 1488–1499.

38. Song, M. H., Iyer, A., Müller-Reichert, T., & O'Connell, K. F. (2008). The Conserved Protein SZY-20 opposes the Plk-4-related Kinase ZYG-1 to limit Centrosome Size. *Developmental Cell*, *15*(6), 901–912.
39. Weng, H., Kim, C., Valavanis, C., et al. (2009). Acheron, an novel LA antigen family member, binds to cask and forms a complex with id transcription factors. *Cellular and Molecular Biology Letters*, 14(2) 273-287.

40. Ohndorf, U.M., Steegborn, C., Knijff, R., Sondermann. P. (2001). Contributions of the Individual Domains in Human La Protein to Its RNA 3'-End Binding Activity. *Journal of Biological Chemistry*, 276(29) 27188 - 27196.

41. Valavanis, C., Wang, Z., Sun, D., Vaine, M., & Schwartz, L. M. (2007). Acheron, a novel member of the Lupus Antigen family, is induced during the programmed cell death of skeletal muscles in the moth *Manduca sexta*. *Gene*. *393*(1-2), 101–109.

42. Wang, Z., Glenn, H., Brown, C., Valavanis, C., Liu, J.-X., Seth, A., Thomas, J.E., Karlstrom, R.O., Schwartz, L.M. (2009). Regulation of muscle differentiation and survival by Acheron. *Mechanisms of Development,* 126(8) 700-709.

43. Cai, L., Fritz, D., Stefanovic, L., & Stefanovic, B. (2010). Binding of Larp6 to the conserved 5' Stem-loop regulates translation of mRNAs encoding type I collagen. *Journal of Molecular Biology*, *395*(2), 309–326.

44. Markert, A., Grimm, M., Martinez, J., Wiesner, J., Meyerhans, A., Meyuhas, O., … Fischer, U. (2008). The La-related protein LARP7 is a component of the 7SK ribonucleoprotein and affects transcription of cellular and viral polymerase II genes. *EMBO Reports*, *9*(6), 569–575.

45. Diribarne, G., Bensaude, O. (2009). 7SK RNA, a non-coding RNA regulating P-TEFb, a general transcription factor. *RNA Biology,* 6(2) 122–128.

46. Okamura, M., Inose, H., Masuda, S. (2015). RNA Export through the NPC in Eukaryotes. *Genes*, 6(1) 124–149.

47. Levesque, L., Guzik, B., Guan, T., Coyle, J., Black, B.E., Rekosh, D., Hammarskjold, M.L., Paschal, B.M. (2001). RNA export mediated by tap involves NXT1-dependent interactions with the nuclear pore complex. *Journal of Biological Chemistry,* 276(48) 44953–44962.

48. Englmeier, L., Fornerod, M., Bischoff, F. R., Petosa, C., Mattaj, I. W., & Kutay, U. (2001). RanBP3 influences interactions between CRM1 and its nuclear protein export substrates. *EMBO Reports*, *2*(10), 926–932.
49. Brennan, C. M., Gallouzi, I.-E., & Steitz, J. A. (2000). Protein Ligands to Hur Modulate Its Interaction with Target Mrnas in Vivo. *The Journal of Cell Biology*, *151*(1), 1–14.

50. Topisirovic, I., Siddiqui, N., Lapointe, V. L., Trost, M., Thibault, P., Bangeranye, C., … Borden, K. L. B. (2009). Molecular dissection of the eukaryotic initiation factor 4E (eIF4E) export-competent RNP. *The EMBO Journal*, *28*(8), 1087–1098.

51. Yang, J., Bogerd, H.P., Wang, P.J., Page, D.C., Cullen, B.R. (2001). Two closely related human nuclear export factors utilize entirely distinct export pathways. *Molecular Cell*, 8(2) 397–406.

52. Kohler, A., Hurt, E. (2007). Exporting RNA from the nucleus to the cytoplasm. *Nature Reviews Molecular Cell Biology.* 8(10) 761–773.

53. Ohno, M., Segref, A., Bachi, A., Wilm, M., Mattaj, I.W. (2000). PHAX, a mediator of U snRNA nuclear export whose activity is regulated by phosphorylation. *Cell*, 101(2) 187–198.

54. Murthi, A., Shaheen, H. H., Huang, H.-Y., Preston, M. A., Lai, T.-P., Phizicky, E. M., & Hopper, A. K. (2010). Regulation of tRNA Bidirectional Nuclear-Cytoplasmic Trafficking in **Saccharomyces cerevisiae**. *Molecular Biology of the Cell*, *21*(4), 639–649.

55. Hopper, A.K., Schultz, L.D., Shapiro, R.A. (1980). Processing of intervening sequences: A new yeast mutant which fails to excise intervening sequences from precursor tRNAs. *Cell,* 19(3) 741–751.

56. Hurt, D. J., Wang, S. S., Lin, Y. H., & Hopper, A. K. (1987). Cloning and characterization of LOS1, a Saccharomyces cerevisiae gene that affects tRNA splicing. *Molecular and Cellular Biology*, *7*(3), 1208–1216.

57. Hunter, C. A., Aukerman, M. J., Sun, H., Fokina, M., & Poethig, R. S. (2003). *PAUSED* Encodes the Arabidopsis Exportin-t Ortholog. *Plant Physiology*, *132*(4), 2135–2143.

58. Li, J., & Chen, X. (2003). *PAUSED*, a Putative Exportin-t, Acts Pleiotropically in Arabidopsis Development But Is Dispensable for Viability. *Plant Physiology*, *132*(4), 1913–1924.
59. Lippai, M., Tirián, L., Boros, I., Mihály, J., Erdélyi, M., Belecz, I., … Szabad, J. (2000). The Ketel gene encodes a Drosophila homologue of importin-beta. *Genetics*, *156*(4), 1889–1900.

60. Shaheen, H. H., Horetsky, R. L., Kimball, S. R., Murthi, A., Jefferson, L. S., & Hopper, A. K. (2007). Retrograde nuclear accumulation of cytoplasmic tRNA in rat hepatoma cells in response to amino acid deprivation. *Proceedings of the National Academy of Sciences of the United States of America*, *104*(21), 8845–8850.

61. Barhoom, S., Kaur, J., Cooperman, B. S., Smorodinsky, N. I., Smilansky, Z., Ehrlich, M., & Elroy-Stein, O. (2011). Quantitative single cell monitoring of protein synthesis at subcellular resolution using fluorescently labeled tRNA. *Nucleic Acids Research*, *39*(19), e129. http://doi.org/10.1093/nar/gkr601

62. Miyagawa, R., Mizuno, R., Watanabe, K., Ijiri, K. (2012). Formation of tRNA granules in the nucleus of heat-induced human cells*. Biochemical and Biophysical Research Communications*, 418(1) 149–155.

63. Hopper, A. K. (2013). Transfer RNA Post-Transcriptional Processing, Turnover, and Subcellular Dynamics in the Yeast *Saccharomyces cerevisiae*. *Genetics*, *194*(1), 43–67.

64. Kramer, E. B., & Hopper, A. K. (2013). Retrograde transfer RNA nuclear import provides a new level of tRNA quality control in *Saccharomyces cerevisiae*. *Proceedings of the National Academy of Sciences of the United States of America*, *110*(52), 21042–21047.

65. Alfano, C., Sanfelice, D., Babon, J., Kelly, G., Jacks, A., Curry, S. (2004). Structural analysis of cooperative RNA binding by the La motif and central RRM domain of human La protein. *Nature Structure and Molecular Biology,* 11(4), 323-329.

APPENDICES

Appendix A: Calculating Protein Concentration

Quantifying a protein using known BSA standards also you to determine a quantity of protein in µg/µL. This value can then be converted in µM concentration using the equation below:

$$\text{Protein Concentration in µM} = \frac{\text{[Protein quantity in g/L]}}{\text{48000g/mol (MW of hLa)}}$$

Appendix B: Calculating Percentage of Protein Bound

To generate a binding curve using Graphpad prism software a percent of protein bound was plotted against the respective protein concentration. The calculation performed to determine percent bound was:

$$\text{Percent protein bound} = \frac{\text{RNA Bound}}{\text{(RNA Bound + RNA Unbound)}} \times 100$$

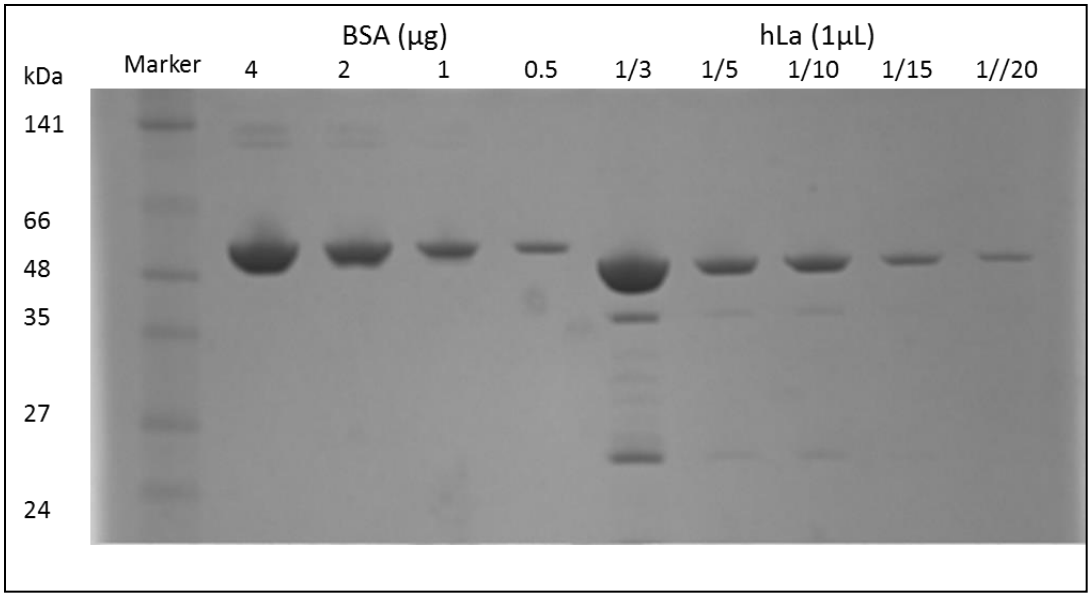

Appendix C: SDS-PAGE of hLa stock dilutions compared against known BSA standards to estimate quantitiy of hLa present in stock. Samples were run on a 10% gel at 120mV.

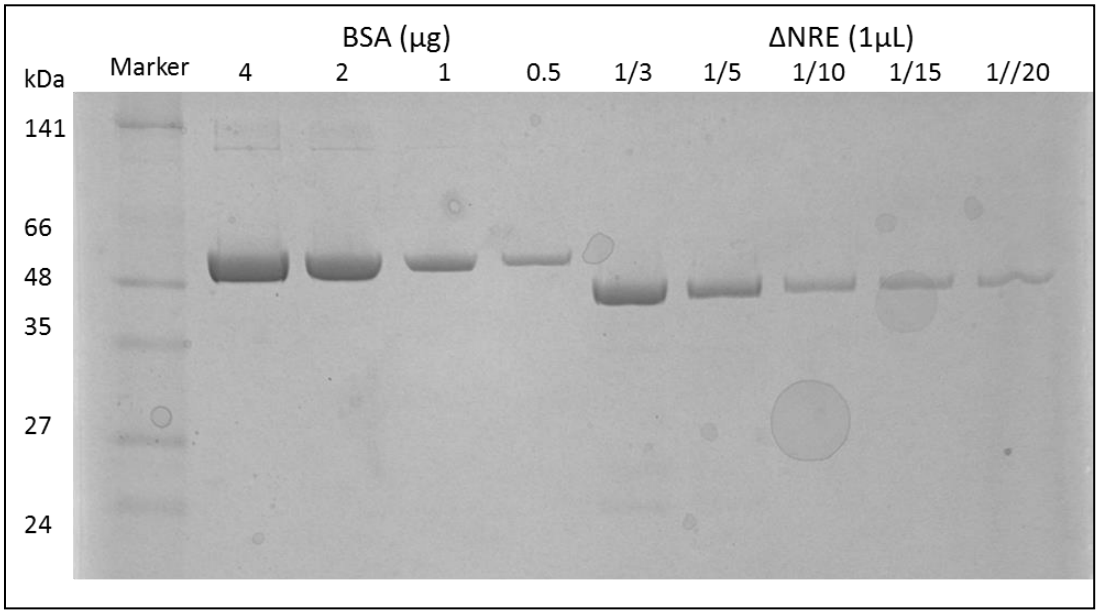

Appendix D: SDS-PAGE of hLa-ΔNRE dilutions compared with known BSA standards to estimate quantity of hLa-ΔNRE in eluted stock. Samples were run on a 10% gel at 120mV.

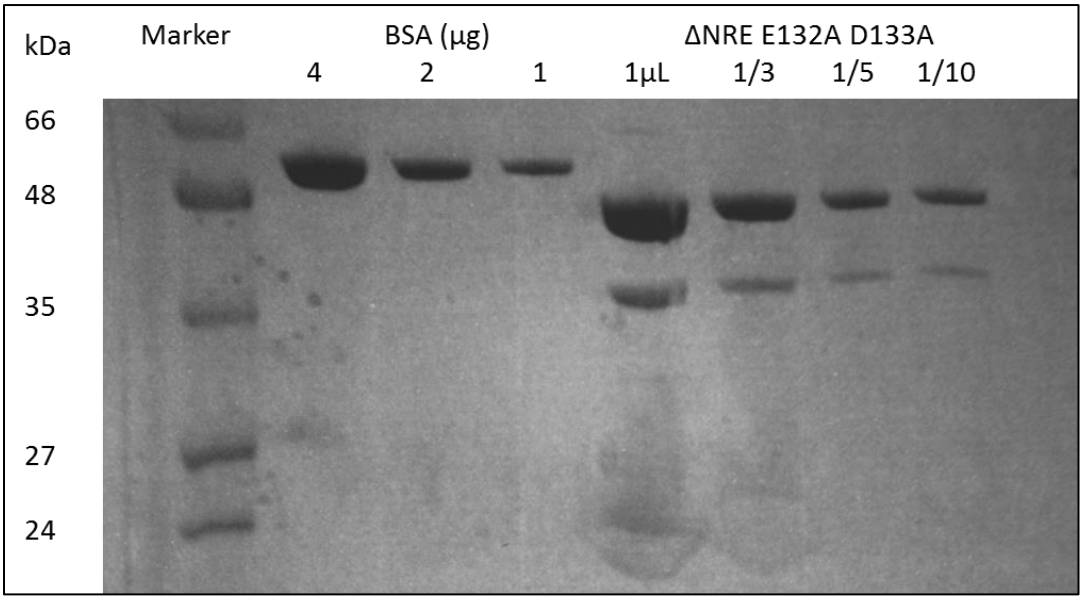

Appendix E: SDS-PAGE of ΔNRE E132A D133A dilutions compared with known BSA standards to estimate quantity in eluted stock. Samples were run on a 10% gel at 120mV.

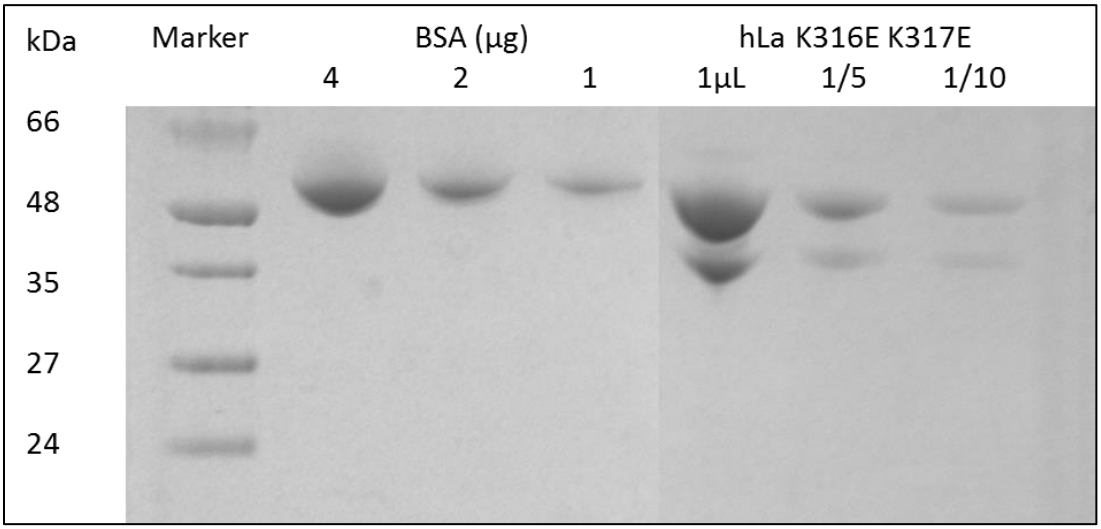

Appendix F: SDS-PAGE of hLa K316E K317E dilutions compared with known BSA standards to estimate quantity of protein in eluted stock. Samples were run on a 10% gel at 120mV

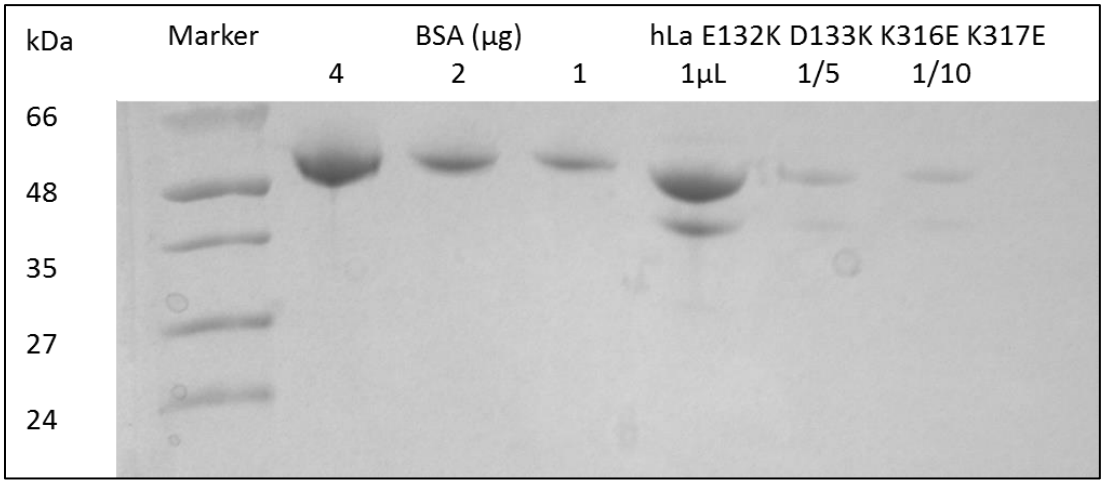

Appendix G: SDS-PAGE of ΔNRE E132K D133K K316E K317E dilutions compared with known BSA standards to estimate quantity of hLa-ΔNRE in eluted stock. Samples were run on a 10% gel at 120mV.

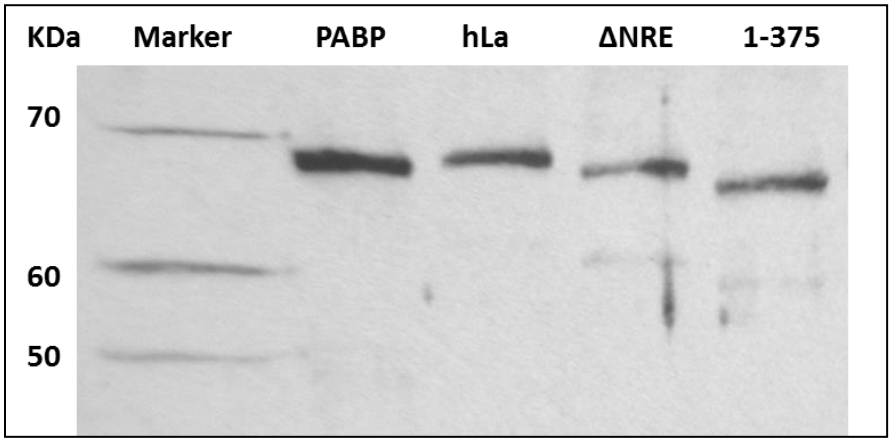

Appendix H: Western blot of the transfection of c-myc tagged PABP and GFP tagged hLa, NRE and 1-375 into Hek293T cells.

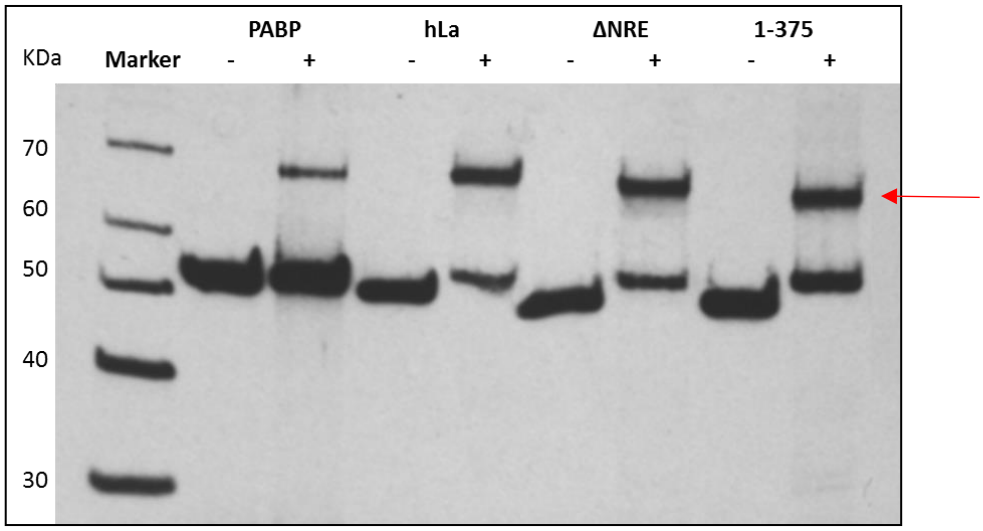

Appendix I: Western blot of the immunoprecipitation of c-myc tagged PABP and GFP tagged hLa, NRE and 1-375. 6ug of control IgG antibody incubated with lysate in (-) lanes and 6 ug of c-myc and GFP antibody incubated with lysate in (+) lanes.